Contrasting roles of the innate receptors TREM2 versus Mincle in the recognition and response of macrophages to mycolic acid-containing lipids in mycobacterial cell walls

Ei'ichi Iizasa
Graduate School of Medical and Dental Sciences, Kagoshima University https://orcid.org/0000-0002-0081-6005

Yasushi Chuma
Japan BCG Laboratory

Takayuki Uematsu
Kitasato University Medical Center https://orcid.org/0000-0002-3680-7231

Mio Kubota
Saga University

Hiroaki Kawaguchi
Graduate School of Medical and Dental Sciences, Kagoshima University

Masayuki Umemura
University of the Ryukyus

Kenji Toyonaga
Osaka University

Hideyasu Kiyohara
Japan BCG Laboratory

Ikuya Yano
Osaka City University Graduate School of Medicine

Marco Colonna
Washington University School of Medicine https://orcid.org/0000-0001-5222-4987

Masahiko Sugita
Kyoto University

Goro Matsuzaki
Tropical Biosphere Research Center, University of the Ryukyus

Sho Yamasaki
Osaka University

Hiroki Yoshida
Saga University https://orcid.org/0000-0003-3447-117X

Hiromitsu Hara (harah@m2.kufm.kagoshima-u.ac.jp)

Graduate School of Medical and Dental Sciences, Kagoshima University

Article

Keywords: ITAM-coupled receptor, mycolic acid, mycobacteria, tuberculosis, TREM2, Mincle, CARD9, immune evasion, innate immunity, macrophage

Posted Date: July 9th, 2020

DOI: https://doi.org/10.21203/rs.3.rs-37581/v1

Version of Record: A version of this preprint was published at Nature Communications on April 16th, 2021. See the published version at https://doi.org/10.1038/s41467-021-22620-3.

Abstract

Mycobacterial cell-wall glycolipids elicit an anti-mycobacterial immune response via FcRγ-associated C-type lectin receptors, including Mincle, and caspase-recruitment domain family member 9 (CARD9). Additionally, mycobacteria harbor immuno-evasive cell-wall lipids associated with virulence and latency; however, their mechanism of action remains unclear. Here, we show that the DAP12-associated triggering receptor expressed on myeloid cells 2 (TREM2) recognizes mycobacterial cell-wall mycolic acid (MA)-containing lipids and suggest a mechanism by which mycobacteria control host immunity via TREM2. Macrophages responded to glycosylated MA-containing lipids in a Mincle/FcRγ/CARD9-dependent manner to produce inflammatory cytokines and recruit inducible nitric oxide synthase (iNOS)-positive mycobactericidal macrophages. Conversely, macrophages responded to non-glycosylated MAs in a TREM2/DAP12-dependent but CARD9-independent manner to recruit iNOS-negative mycobacterium-permissive macrophages. Furthermore, TREM2 deletion enhanced Mincle-induced macrophage activation in vitro and inflammation in vivo and accelerated the elimination of mycobacterial infection, suggesting that TREM2-DAP12 signaling counteracts Mincle-FcRγ-CARD9-mediated anti-mycobacterial immunity. Mycobacteria, therefore, harness TREM2 for immune evasion.

Introduction

Tuberculosis (TB) is a chronic infectious disease caused by *Mycobacterium tuberculosis* (*Mtb*) and remains a major cause of morbidity and mortality worldwide. Most infected individuals do not manifest clinical symptoms of TB (referred to as latent infection). In this phase, the bacteria are dormant with a non-replicating phenotype and resistant to reactive intermediates and antibiotics, consistently evading host immune recognition 1.

A distinctive trait of mycobacteria is their highly lipid-rich outer membrane, which is not only critical for their replication, acid-fast properties, and drug resistance, but also plays a key role in pathogenicity2,3 Some of these lipids trigger immunopathologic response, whereas others have immuno-evasive functions associated with virulence and latency4. Mycolic acids (MAs) are mycobacterium and related spp.-specific lipids with extremely long fatty acids (C_{60}-C_{90}) and represent predominant component in mycobacterial cell-walls. MAs form the cell wall skeleton by covalently linking to the arabinogalactan (ABG) and peptidoglycan (PG) basement layer and also exist on the cell wall surface in either glycosylated or non-glycosylated forms5. Their composition is altered dynamically depending on mycobacterial life-cycle stage and external environmental conditions6,7, and this affects bacterial virulence and latency by controlling host immunity. For example, glycosylated MA-containing lipids, such as trehalose dimycolate (TDM; also known as cord factor) and glucose monomycolate (GMM), possess potent pro-inflammatory and adjuvant activity and are capable of inducing lung granulomas when injected into animals8,9. These glycolipids are predominantly synthesized in actively replicating mycobacteria, while their levels are markedly diminished in dormant mycobacteria6. Non-glycosylated MA lipids, such as free MA (fMA) and glycerol monomycolate (GroMM), are associated with mycobacterial persistence, immune suppression, and biofilm formation. fMA is increased in cell walls in

non-replicating persistent mycobacteria6, forms biofilms10,11, and also inhibits cytokine production and phagosome-lysosome fusion in macrophages. A hypervirulent mutant *Mtb* strain (Δ*mce1*) with a disruptied *mce1* operon, which results in excess accumulation of fMA in the cell wall12,13, induces a weak macrophage chemokine response14, fails to elicit a strong Th1 response, and causes poorly organized lung granulomas in mice13, relative to that of the wild-type strain. GroMM is associated with latent infection15 and induces eosinophilic inflammation and T helper (Th)2-type cytokine production16, which might counteract Th1-mediated anti-mycobacterial immunity. However, the molecular mechanisms by which these non-glycosylated MA lipids modulate host immunity remain unclear.

Although pathogen recognition by macrophages usually triggers the immune responses that eliminate the pathogens, macrophages are the primary target cells of *Mtb* and serve as an intracellular niche for *Mtb* propagation and latency17. *Mtb* has evolved remarkable immune-evasion strategies that enable intracellular persistence in macrophages18. The cell-wall lipids phthiocerol dimycocerosates (PDIMs) and the structurally related phenolic glycolipids (PGLs) represent virulence factors found only in a limited subset of pathogenic mycobacteria, such as hyper-virulent W-Beijing strains of *Mtb*19. The surface expression of these lipids on mycobacteria masks ligands for toll-like receptors (TLRs) that are required for the induction of inducible nitric oxide synthase (iNOS)-positive M1-type microbicidal macrophages, and instead recruits iNOS-negative non-microbicidal macrophages (referred to as “permissive macrophages”) to the site of infection, thereby facilitating intracellular *Mtb* survival and propagation20. The recruitment of permissive macrophages is dependent on CCR2 and the induction of its ligand monocyte chemoattractant protein-1 [MCP-1 (CCL2)] by PGL through activation of the STING cytosolic sensing pathway20,21.

Evidence for the importance of immunoreceptor tyrosine-based activation motif (ITAM)-coupled receptors, including C-type lectin receptors (CLRs) and immunoglobulin superfamily receptors, is accumulating with regard to innate immunity against a variety of pathogens22–25. These receptors associate with the ITAM-bearing signaling adaptors DAP12 or FcRγ, or harbor cytoplasmic ITAM-like motifs called hemITAM for signal transduction26. Ligand recognition by these receptors triggers tyrosine phosphorylation in ITAM, followed by activation of the tyrosine kinase Syk, leading to the downstream activation of mitogen-activated protein kinases (MAPKs) and nuclear factor-kappa B (NF-κB) through the signaling adaptor caspase-recruitment domain family member 9 (CARD9). CARD9 acts in complex with B-cell lymphoma/leukemia-10 (Bcl10) and Mucosa-associated lymphoid-tissue lymphoma- translocation protein-1 (Malt1) and plays an essential role in ITAM-coupled receptor- induced myeloid cell activation26,27. Recent reports highlight the importance of CARD9 and the FcRγ-associated CLRs, which recognize mycobacterial cell wall glycolipids, in anti-mycobacterial innate immunity28. CARD9-deficient mice are highly susceptible to *Mtb* infection29. Mincle (Clec4e) recognizes TDM to elicit pulmonary inflammation and induces granuloma formation in an FcRγ-dependent manner30. MCL (Dectin-3/Clec4d) also recognizes TDM and form a dimer with Mincle to stabilize its surface expression31,32. Dectin-2 (Clecsf10) recognizes mannose-capped lipoarabinomannan (LAM) and plays a central role in production of IL-10 and IL-2 during mycobacterial infection33. DCAR (mouse clec4b1) recognizes phosphatidylinositol mannosides (PIM) and promotes monocyte recruitments and the Th1 responses34.

In contrast to CLR-associated FcRγ, the other ITAM-bearing signaling adaptor, DAP12, might negatively regulate the anti- mycobacterial immune response, because DAP12 deficiency accelerates the clearance of mycobacteria and the granuloma formation in lungs upon *Mtb* or *Mycobacterium bovis* Bacille de Calmette et Guerin (BCG) infection35,36. These observations implicate unknown DAP12-associated regulatory receptors that might possibly recognize immune- suppressive ligands in mycobacteria. However, these theoretical receptors, as well as the precise mechanisms of immune suppression via DAP12, have not been described.

In the present study, we present evidence suggesting that the DAP12-associated receptor triggering receptor expressed on macrophage 2 (TREM2) recognizes mycobacterial MA-containing lipids that are distinct from those recognized by Mincle and counteracts the Mincle-FcRγ-CARD9-mediated anti-mycobacterial immune response. We show that the glycosylated MA-containing lipids induce mycobactericidal macrophages in a Mincle/FcRγ/CARD9-dependent manner. Conversely, the non-glycosylated MA-containing lipids induce mycobacteria-permissive macrophages in a TREM2/DAP12-dependent but CARD9-independent manner. Moreover, loss of TREM2 markedly enhances Mincle-induced macrophage activation *in vitro* and inflammation *in vivo* and accelerated the elimination of mycobacterial infection in mice. These results suggest that mycobacteria evade host immunity via TREM2 to avoid mycobactericidal macrophage activation through the Mincle-CARD9 pathway. This finding describes a mechanism by which mycobacteria controls the host immune response through a host regulatory innate immune receptor, which may have implications for treatment of mycobacteriosis including TB.

Results

TREM2 recognizes mycobacteria

To screen novel ITAM-coupled receptors capable of recognizing mycobacteria, we analyzed the binding of 20 known ITAM-coupled CLR, TREM, and leukocyte mono-Ig- like receptor (LMIR; CD300) family receptors22,37–39 fused to Fc-antibody fragments to heat-killed mycobacterial strains, including the virulent strain *Mtb* H37Rv, the attenuated strain *Mtb* H37Ra, and the vaccine strain *M. bovis* BCG, using flowcytometry. In addition to several CLRs previously reported to recognize mycobacteria, including Mincle, specific ICAM-3 grabbing nonintegrin-related (SIGNR)1, SINGNR3, and DC-SIGN30,40, this screening identified TREM2 and LMIR5 as novel receptors capable of binding to mycobacteria (Fig. 1a). Especially, TREM2 demonstrated a strong binding capacity to all tested mycobacterial strains, which prompted us to further characterize this interaction.

To investigate whether recognition of mycobacteria by TREM2 activates intracellular ITAM signaling, we used nuclear factor of activated T cells (NFAT)-driven green fluorescent protein (GFP)-reporter cells (2B4)30 ectopically expressing TREM2 and its signaling subunit DAP1241,42. As reported previously30, *Mtb* H37Rv, *Mtb* H37Ra, and M. *bovis* BCG stimulated NFAT-GFP signaling in reporter cells expressing Mincle and FcRγ (Supplementary Fig. 1a). We found that all these mycobacterial strains clearly activated

reporter cells expressing TREM2 and DAP12, but not in those expressing only DAP12, in a dose dependent manner (Fig. 1b). Whereas, none of these strains activate reporter cells expressing TREM1 plus DAP12 (Supplementary Fig. 1b). Importantly, the level of stimulation by TREM2 and Mincle differed between the strains (Fig. 1b and supplementary Fig. 1a), suggesting that TREM2 and Mincle recognize different ligands commonly expressed by these mycobacterial strains.

TREM2 recognizes MAs

TREM2 binding to mycobacteria implies that its ligand(s) exist on the cell-wall surface, where mycobacteria express a wealth of unique lipids that influence the host immune responses 43. Given that TREM2 binds to various endogenous mammalian lipids44,45, we first examined whether mycobacterial lipids contain TREM2 ligand(s). De-lipidation of *Mtb* H37Ra with chloroform and methanol (C:M) (Fig. 2a) markedly diminished the level of stimulation in TREM2-reporter cells (Fig. 2b), as well as in Mincle-reporter cells as reported30 (Fig. 2c). Accordingly, the lipid-containing C:M fraction (Fig. 2a) but not the hydrophilic M:W fraction showed strong stimulating activity in TREM2 reporter cells (Fig. 2b) as with Mincle reporter cells (Fig. 2c), implicating that TREM2 ligands were present in the cell wall lipid fraction as with so Mincle ligands 30. We then next tested the TREM2-stimulating activity using known major constituents of mycobacterial cell wall, including the glycans PGN and AbG, the immunostimulatory glycolipids LAM and TDM (Fig. 2d), and fMA (Fig. 2d). We observed that AbG, PGN, and LAM did not activate the TREM2-reporter cells, even at higher concentrations (Fig. 2e-g), whereas we observed substantial ligand activity with TDM and fMA (Fig. 2h). Importantly, loss of trehalose moiety from TDM (i.e. fMA) markedly increased the TREM2-stimulating activity (Fig. 2h), while it completely abolished the Mincle-stimulating activity as reported (Fig. 2i)30. These results suggest that TREM2 recognizes the MA moiety of TDM, and that the sugar moiety interferes with this recognition.

We then investigated the structure of MA necessary for TREM2 recognition. Extremely long (C_{60}-C_{90}) and branched alkyl chains are hallmarks of mycobacterial MAs. To assess the importance of the length and branching, we compared the stimulatory activity of mycobacterial MA with that of *Rhodococcus equi (R. equi*) MA, which has shorter alkyl chains (C_{35}), and of behenic acid (BA), which is a linear fatty acid with an alkyl chain (C_{22}) of similar length with the mero-chain of *R. equi* MA (Fig. 2j). *R. equi* MA exhibited a similar level of stimulatory activity in TREM2-reporter cells as mycobacterial MA, whereas the level of stimulation with BA was very low, even at higher concentrations of BA (Fig. 2j), suggesting that the branched structure rather than the alkyl-chain length was important for TREM2 recognition of MA. To further investigate this, we tested the ligand activity of palmitic acid (PA; C_{16}), 2-tetradecylhexadecanoic acid (THA) (C_{14}/C_{16}), which bears a PA-based synthetic fatty-acid with similar branching structure as MA but lacking its 3-hydroxyl residue, and 3-hydroxybutyric acid (HBA), which has only the carboxyl and hydroxyl residue at the branching moiety of MA (Fig. 2k). We detected TREM2 stimulation with THA, albeit at a lower level than MA, but could not detect stimulation with PA and HBA (Fig. 2k), suggesting that TREM2 recognition requires a branched fatty acid structure with an alkyl chain.

The R47H mutation in TREM2, which is associated with a higher risk of several neurodegenerative diseases46–49, impairs the recognition of brain lipids45,50. We found that the TREM2 R47H mutation also attenuated MA recognition (Supplementary Fig. 2), suggesting that this residue is important for MA recognition by TREM2.

TREM2 and Mincle preferentially recognize distinct MA-containing lipids based on their glycosylation

Mycobacteria express a variety of MA-containing lipids on their cell wall51. Since both Mincle and TREM2 have the capacity to recognize MA-containing lipids, we next compared their binding activity to the glycosylated (TDM and GMM) or the non-glycosylated (GroMM and fMA) MA-containing lipids (Fig. 3a) using the receptor-Fc fusion proteins. We observed that Mincle-Fc not only showed strong binding to TDM as expected, but also binding to GMM, whereas it showed no detectable binding to fMA and weak binding to GroMM only at higher concentrations (Fig. 3b). By contrast, TREM2- Fc showed strong binding to GroMM and fMA but showed relatively much weaker binding to TDM and GMM (Fig. 3b). We then examined whether the different binding of MA-containing lipids to TREM2 and Mincle reflect their receptor-stimulatory activities using NFAT-GFP-reporter cells. Consistent with the binding data, TREM2-reporter cells strongly responded to MA and GroMM but weakly to TDM and GMM, whereas Mincle-reporter cells responded strongly to TDM and GMM but weakly to GroMM only at higher concentrations and did not respond to fMA (Fig. 3c). Therefore, TREM2 and Mincle preferentially recognize non-glycosylated and glycosylated MA-containing lipids, respectively.

Glycosylated and non-glycosylated MAs elicit distinct macrophage activation through Mincle and TREM2

To investigate the relevance of TREM2 and Mincle recognition of MA-containing lipids in the activation of innate immune cells, we stimulated peritoneal macrophages from wild-type (WT), TREM2-deficient (*Trem2−/−*), or Mincle-deficient (*Clec4e−/−*) mice with either glycosylated or non-glycosylated MA-containing lipids and examined their production of MCP-1, a pivotal monocyte chemoattractant implicated in TB pathology52– 54, and TNF, an essential cytokine for granuloma formation and TB control55,56. Interestingly, we found that activation of WT macrophages by the glycosylated MA-containing lipids TDM or GMM or by lipopolysaccharide (LPS) induced production of both MCP-1 and TNF, whereas activation of macrophages with the non-glycosylated MA-containing lipids GroMM or fMA induced production of MCP-1 but not TNF (Fig. 4a), as well as other pro-inflammatory cytokines, including IL-6 and IL-12p40 (Supplementary Fig. 3a). Loss of Mincle almost completely abolished TNF, as previously30, as well as MCP-1 in response to TDM as expectedly30. We found that Mincle deficiency also abolished these productions induced by GMM (Fig. 4a). However, Mincle deficiency did not affect MCP-1 production in response to GroMM or fMA. By contrast, loss of TREM2 almost completely abolished the MCP-1 production in response to GroMM or MA, but not to TDM or GMM (Fig. 4a). These results demonstrated that glycosylated and non-glycosylated MA-containing lipids elicited distinct macrophage activation, which was dependent on Mincle and TREM2, respectively.

Triggering of ITAM-coupled receptors on myeloid cells activates the ITAM-Syk-CARD9 signaling pathway to induce cytokine production57. To investigate whether MCP-1 and TNF production induced by MA-

containing lipids depends on this pathway, we first confirmed the requirement for DAP12 and FcRγ, which are the ITAM-containing signaling subunits of TREM2 and Mincle, respectively. As expected, we observed that FcRγ-deficient (*Fcer1g−/−*) and DAP12-deficinet (*Tyrobp−/−*) macrophages almost phenocopied Mincle-deficient and TREM2-deficient macrophages, respectively, with similar patterns of defects in TNF and MCP-1 productions in response to glycosylated or non-glycosylated MA-containing lipids (Fig. 4b). However, FcRγ deficiency slightly dampened MCP-1 induction by fMA or GroMM at higher concentrations, implicating that FcRγ might partly contribute to TREM2 signaling. We then examined the requirement for Syk and CARD9 for each of these responses. Treatment of WT macrophages with a Syk inhibitor (BAY-613606) abrogated both MCP-1 and TNF production in response to all MA-containing lipids (Fig. 4c), indicating essential role for Syk in the response to these lipids. Intriguingly, although TNF production induced by glycosylated MAs through Mincle was abolished in CARD9-deficient (*Card9−/−*) macrophages, as expected58, CARD9-deficiency did not affect MCP-1 production induced by both glycosylated and non-glycosylated MA-containing lipids (Fig. 4c). Collectively, these results demonstrated that mycobacterial MA-containing lipids induced TNF production through Mincle via the canonical FcRγ-Syk-CARD9 pathway, while they induced MCP-1 production via the ITAM-Syk pathway but independent of CARD9 signaling (Supplementary Fig. 3b).

TREM2/DAP12 signal inhibits macrophage activation through Mincle/FcRγ

Interestingly, we observed that loss of TREM2 markedly enhanced MCP-1 and TNF production by peritoneal macrophages in response to TDM or GMM (Fig. 4a). This was also true in *Tyrobp−/−* macrophages (Fig. 4b), suggesting an inhibitory role of TREM2/DAP12 signaling in Mincle/FcRγ-induced macrophage activation. We did not observe an increase in cytokine response when the same preparation of *Trem2−/−* macrophages were stimulated with TLR ligands, such as Pam_3CSK_4 (for TLR2), LPS (for TLR4), Poly (I:C) (for TLR3), CpG-ODN (for TLR9), or with the Dectin-1 ligand zymozan (Fig. 4a and supplementary Fig. 4a, b). This selective enhancement of Mincle activation in the absence of TREM2 was more prominent in BMDMs, where TDM- induced TNF was detected at very low levels in WT BMDMs. Nevertheless, *Trem2−/−* or *Tyrobp−/−* BMDMs showed substantial TNF production in response to TDM (Supplementary Fig. 4c), whereas this enhancement was not observed following Pam_3CSK_4 or LPS stimulation. Additionally, we observed an increased cytokine response following stimulation of *Trem2−/−* BMDMs with mycobacterial total lipids (C:M fraction in Fig. 2a) prepared from *Mtb* R37Ra or *M. bovis* BCG (Supplementary Fig. 4d). This response was largely dependent on Mincle, as *Clec4e−/−* BMDMs produced markedly lower TNF in response to the total lipids compared to WT BMDMs (Supplementary Fig. 4d). These data clearly indicated that TREM2/DAP12 signaling selectively inhibited macrophage activation induced by Mincle-FcRγ signaling.

Triggering of TREM2 induces permissive macrophages

Given that NO plays a pivotal role in controlling mycobacterial infections59,60, we investigated the action of TREM2 and Mincle on NO production by macrophages. We observed that TDM stimulation strongly induced NO production by bone marrow-derived macrophages (BMDMs), as reported previously30, while

fMA did not substantially induce NO production (Fig. 5a). This was consistent with the observed increase in *Nos2* expression, which encodes iNOS, after stimulation with TDM but not fMA (Supplementary Fig. 5a). Additionally, the TDM-induced NO production by macrophages was inhibited following the addition of a TNF blocking antibody (Fig. 5b). Inversely, addition of recombinant TNF to the fMA-stimulated culture induced NO production by macrophages (Fig. 5b), indicating that NO production was dependent on TNF, which is consistent with previous findings61–63.

We then characterize the inflammation triggered via Mincle and TREM2 *in vivo*. Because TDM induces lung granulomas in mice via the Mincle/FcRγ pathway30, we examined whether fMA had a similar effect. Intravenous injection of a TDM (oil-in- water) emulsion into mice induced massive granulomatous lesions in the lungs, which was completely abolished in *Clec4e−/−* mice (Fig. 5c), as reported previously30. Additionally, this effect was also absent in *Card9−/−* mice, indicating that TDM-induced granuloma formation was dependent on Mincle/CARD9 signaling. By contrast, we did not observe lung granulomatous lesions in mice injected with an fMA emulsion (Fig. 5c), suggesting that fMA cannot activate CARD9 signaling. To further explore the innate immune response induced by TDM or MA *in vivo*, we intraperitoneally injected the TDM or fMA emulsion into mice and measured the level of MCP-1 and TNF, and *Nos2* mRNA levels, as well as the number of recruited inflammatory cells, induced in the peritoneal cavities. We detected MCP-1 in peritoneal lavages following respective fMA and TDM administrations at similar levels, with peak MCP-1 levels observed at 4- and 24-h post- injection, respectively (Fig. 5d). However, TNF production and *Nos2* mRNA expression were induced only by TDM but not fMA (Fig. 5d), which was consistent with results from the *in vitro*-stimulated macrophages (Fig. 4). Moreover, we observed that TDM recruited substantial numbers of macrophages [CD11b+Ly6G− F4/80low small peritoneal macrophages (SPMs)], Supplementary Fig. 5b) and neutrophils (CD11b+Ly6G+ F4/80−, Supplementary Fig. 4b) to the cavity, whereas fMA recruited comparable numbers of macrophages as TDM but fewer neutrophils only immediately after administration (Fig. 5e). Importantly, MCP-1 level (Fig. 5f) and the number of recruited cells (Fig. 5g) induced by fMA in *Trem2−/−* mice were almost the same as those induced by the control vehicle administration, indicating that the fMA-induced inflammation was dependent on TREM2.

To investigate the phenotype of TDM- or fMA-induced macrophages, we examined the expression of the inflammatory M1-macrophage markers iNOS and CD38 64 in the recruited macrophages (Fig. 5h). Intraperitoneal administration of TDM and fMA recruited comparable numbers of macrophages to the cavity (Fig. 5i); however, although TDM-induced macrophages exhibited a CD38highiNOS+ phenotype (Fig. 5j), those induced by fMA had reduced CD38 expression and were negative for iNOS (Fig. 5k). This phenotype resembles a previously reported phenotype associated with permissive macrophages that are recruited by a subset of pathogenic mycobacteria expressing the virulence lipids PDIM and PGL in an MCP-1 and CCR2-dependent manner and provide a niche for mycobacterial propagation21,65.

Collectively, these results suggested that triggering of the Mincle-CARD9 pathway elicited lung granuloma formation and recruited M1-type mycobactericidal macrophages producing TNF and NO, whereas TREM2 activation recruited mycobacterium-permissive macrophages lacking TNF and NO production.

TREM2 deficiency exacerbates Mincle-induced inflammation

To investigate the relevance of TREM2 inhibition of Mincle-induced macrophage activation *in vivo*, we assessed the impact of TREM2 deficiency on tissue inflammation induced by TDM administration. Intraperitoneal injection of TDM emulsion into *Trem2−/−* mice resulted in significantly higher levels of TNF and MCP-1 production and increased *Nos2* mRNA expression (Fig. 6a), as well as higher numbers of macrophages and neutrophils to the peritoneal cavities (Fig. 6b), as compared to those observed in WT mice. Intravenous injection of the TDM emulsion into mice induces lung swelling (increased lung weight index: LWI) and thymic atrophy (decreased thymic weight index: TWI) dependent on the Mincle-FcRγ pathway30. We observed that *Trem2−/−* mice displayed significantly higher LWI and lower TWI than WT mice followingr TDM injection (Fig. 6c). Histopathological analysis of the lungs revealed that the granulomatous lesions were markedly more prominent in *Trem2−/−* mice (Fig. 6d). In addition, specific pathological features in the form of prominent vasculitis and edema, indicating accelerated inflammation, were observed in the lungs of *Trem2−/−*, but not WT mice (Supplementary Fig. 6). Consistent with these results, the levels of TNF and MCP-1 production and *Nos2* mRNA expression in the inflamed lungs were significantly higher in *Trem2−/−* mice than in WT mice (Fig. 6e). These results suggested that TREM2 suppressed Mincle-induced inflammation *in vivo*.

TREM2 deficiency accelerates the clearance of mycobacterial infection

Since our data suggested a suppressive role for TREM2 in the microbicidal innate immune response via Mincle, we investigated the impact of TREM2 deficiency on the clearance of mycobacterial infection. First, we infected WT and *Trem2−/−* BMDMs with *M. bovis* BCG *in vitro* and assessed NO production and mycobacterial killing in the macrophages. NO production in *Trem2−/−* BMDMs was significantly higher than in WT BMDMs (Fig. 7a). Accordingly, the number of intracellular BCG colony-forming units (CFUs) was significantly lower in *Trem2−/−* BMDMs than in WT BMDMs (Fig. 7b). Next, to investigate the relevance of this observation *in vivo,* we intraperitoneally infected WT and *Trem2−/−* mice with *M. bovis* BCG and measured bacterial clearance. The bacterial burden (CFUs) in the peritoneal cavities at day 1 and 3 after infection were significantly lower in *Trem2−/−* mice than in WT mice (Fig. 7c). Consistently, early MCP-1 production (Fig. 7d) and the number of infiltrated macrophages (Fig. 7e) after infection were significantly higher in *Trem2−/−* mice than in WT mice. Moreover, *Nos2* expression in infiltrated cells tended to be higher (Fig. 7f, left), whereas expression of the M2 marker *arginase 1 (Arg1*) was significantly lower in *Trem2−/−* mice (Fig. 7f, right) relative to that in WT mice, suggesting that lack of TREM2 signaling favored M1 polarization. These results suggested that TREM2 contributed to immune evasion by mycobacteria by inhibiting the activation of microbicidal M1 macrophages.

Discussion

In the present study, we identified the DAP12-associated TREM2 as a receptor for mycobacteria by the screening using the ITAM-coupled receptor-Fc fusion protein library. TREM2 is expressed on various myeloid cells, including macrophages and microglia65, and *Trem2* deficiency is reportedly related to

various neurodegenerative diseases. Homozygous loss-of-function mutations of *Trem2* or *dap12* cause Nasu-Hakola disease accompanied by demyelination and axonal loss66,67. Single nucleotide polymorphisms, including the TREM2 R47H variant, increase the risk of dementia, including frontotemporal lobar degeneration, Parkinson's disease, Alzheimer's disease, and amyotrophic lateral sclerosis46–49. These genetic associations highlight the physiological importance of TREM2 and its ligand recognition. Previous reports indicate that TREM2 binds to anionic ligands of bacteria68, lipo-oligosaccharide (LOS) of *Neisseria gonorrhoeae*69,70, several brain lipids associated with fibrillar amyloid β45, and apolipoproteins71. Although these ligands have been identified, ligand structures prerequisites for TREM2 recognition remain unknown. Here, we identified MA- containing lipids as TREM2 ligands and found that their branched alkyl chains are required for TREM2 recognition via a structure-activity relationship analysis. The removal of branched alkyl chains from LOS by O-deacetylation diminishes TREM2-LOS interaction70, which implicates the lipid moiety of LOS in the interaction with TREM2. Additionally, TREM2 ligands in the brain include phospholipids or sphingolipids carrying branched alkyl chains45; therefore, our findings agree with previous results and might offer insight into future searches for unknown TREM2 ligands.

We found that macrophage activation by glycosylated versus non-glycosylated MA lipids resulted in different patterns of response with different receptor requirements. While glycosylated MAs were recognized by Mincle, and induced the production of MCP-1, TNF, and NO, non-glycosylated MAs were recognized by TREM2 and induced only MCP-1 production. A previous report showed that human Mincle but not mouse Mincle could recognizes GroMM and induces TNF production in primary human macrophages72, suggesting that the range of structures of MA ligands recognized by Mincle might differ between humans and mice. Nevertheless, Hattori et al showed in this report that the binding affinity of human Mincle to GroMM was ~100-fold lower than that to TDM, indicating the importance of the sugar moiety for the recognition by Mincle, regardless of species. Importantly, our data showed that mouse Mincle was also capable of binding to GroMM at higher concentrations, although it was not essential for macrophage response to GroMM. Future studies should clarify the contributions of TREM2 and Mincle to recognition of MA-containing lipids in humans.

MCP-1 plays a role in the early stages of *Mtb* infection53,54. Additionally, higher levels of MCP-1 production are associated with greater severity of tuberculosis in human patients73. The polymorphism of at position -2518 the MCP-1 promoter is associated with TB susceptibility74,75, and the odds of developing TB is 2.3- to 5.5-fold higher in patients with MCP-1 genotypes AG and GG relative to those with the AA genotype. Patients carrying the AG or GG genotype harbor extremely high concentrations of MCP-1, which inhibit the expression of IL-1275, suggesting that elevated MCP-1 production and lower inflammatory cytokine levels promote TB development. This is a similar phenomenon to that observed following TREM2 recognition of non-glycosylated MAs in the present study. Mycobacterial cell-wall components, PDIM and PGL, enhance infectivity by selective induction of MCP-1 for the recruitment of the permissive macrophages76. These findings indicate that exclusive production of MCP-1 via TREM2 is presumably beneficial to mycobacteria.

The recruitment of permissive macrophages and inhibition of Mincle-FcRγ- CARD9 signaling are key functions of TREM2. Here, we found that TREM2/DAP12 signaling specifically inhibited Mincle-FcRγ-CARD9 signaling but not TLR signaling. However, previous reports show that TREM2 deficiency enhances cytokine production induced by TLRs77,78. Although the reason for this discrepancy is unknown, upregulated signaling via Mincle might be responsible for the enhanced TLR response. Because Mincle recognizes damaged cell-derived endogenous ligands79,80, Mincle expression induced by TLR stimulation30 might subsequently amplify the TLR response81 depending on cell condition. Alternatively, TREM2 binding to TDM (Figure 3) but not TLR ligands could generate significant inhibitory signals upon TDM stimulation; therefore, TREM2 deficiency might result in more obvious effects on the signaling via Mincle than that via TLRs.

The composition of MA-containing lipids dynamically changes in response to the external environment. TDM is a major glycosylated MA in the mycobacterial cell wall in culture, but in the host under glucose-rich condition, TDM synthesis is downregulated, and GMM is produced by mycolytransferases using host-derived glucose7. Because glycosylated MAs exhibit potent adjuvant activity82, the presence of these lipids preferentially activates the immune response through Mincle to eliminate mycobacteria. Lipid composition differs in latent mycobacterial infections. GroMM might be associated with latent mycobacteria, given that GroMM-reactive T cells are observed only in latent but not active TB cases15,72. Additionally, levels of glycosylated MAs decrease in *Mtb* in a non-replicating dormant-like state6. Therefore, we speculate that the recognition of latent mycobacterial cell walls by TREM2 might lead to the recruitment of permissive macrophages, thereby promoting chronic infection (Supplementary Fig. 7).

Macrophages or microglia phagocytize bacteria or apoptotic cell debris through TREM2 69,83–85. Macrophages are roughly classified into M1 and M2 subtypes that exert opposite effects on the inflammatory response86. M1 macrophages are pro-inflammatory, whereas M2 macrophages are anti-inflammatory and exhibit phagocytic activity to promote tissue repair and homeostasis. Unlike FcRγ-coupled mycobacterial receptors including Mincle, TREM2-DAP12 signaling seemingly confers M2-like anti- inflammatory properties on macrophages. Indeed, IL-4, which skews macrophage polarization toward M2, induces TREM2 expression in macrophages78. Additionally, TREM2 deficiency impairs wound healing of colonic mucosal injures accompanied by diminished M2 differentiation and increased TNF and interferon (IFN)-γ production87. Moreover, TREM2 plays an important role in maintaining homeostasis in the brain by clearance of dead cells or amyloid-β through brain-lipid recognition83. Therefore, mycobacteria presumably harness the functions of TREM2 by stimulating TREM2 with MA-containing lipids to gain niches suitable for their propagation.

Collectively, our data suggest that TREM2-DAP12 signal activation by non- glycosylated MAs, which are associated with virulent or latent mycobacterial infections, recruits permissive macrophages and suppress the mycobactericidal immune response induced by glycosylated MAs through Mincle-FcRγ-CARD9 signaling. Therefore, this study elucidated al mechanism by which mycobacteria control the host immune response by stimulating a host regulatory receptor with their specific cell-wall lipids. Our findings

suggest that targeting the TREM2-DAP12 pathway might represent a novel therapeutic intervention to control mycobacterial diseases.

Methods

Reagents

MA from *M. bovis* BCG was prepared as described below. TDM, LPS, ABG, PA and HBA were purchased from Sigma-Aldrich. Poly (I:C), CpG-ODN, Pam3CSK were purchased from InvivoGen. Oxidized (OX)-zymosan was kindly provided by Prof. Naohito Ohno (Tokyo University of Pharmacy and Life Sciences). MA from *R. equi* was kindly provided by Dr. Jun Miyazaki (Tsukuba University). LAM was purchased from Nakalai tesque. THA was purchased from Wako pure chemical industries. GMM and GroMM were prepared as described previously 7,16 and the final preparations provided no extra spots on analytical TLC plates, and the identity of the lipids was confirmed by mass spectrometry.

Preparation of MA

Free MAs were isolated from heat-killed *M. bovis* BCG (Tokyo 172 strain). The BCG cells were suspended in 85% tetrahydrofuran (THF)/water solution under a nitrogen atmosphere, followed by reflux with stirring for 1 h. The cell suspension was filtrated under pressure and washed with 75% THF/water solution. The residue was resuspended in 75% THF/water solution under a nitrogen atmosphere, followed by reflux with stirring for 1h. The suspension was filtrated under pressure and washed with 75% THF/water solution three times and with methanol twice. Then, the bacterial cells were suspended in 50% 2-propanol/water solution containing 10% potassium hydroxide, followed by reflux with stirring for 2 h to complete alkaline hydrolysis of MA ester. After the refluxing, the suspension was cooled down on ice, and acidified with 6 M hydrochloric acid. The reaction mixture was extracted twice with *n*-heptane, and the *n*-heptane fraction was washed twice with water and then twice with 90% ethanol/water. Finally, the *n*-heptane fraction was concentrated *in vacuo* to obtain purified MAs. The product was applied for TLC (*n*-hexane:methyl *tert*-butyl ether: formic acid = 8/2/0.5, v/v/v) to confirm no extra no spots and for MADI-TOF mass spectrometry analyses to confirm the identity of MAs.

Mice

All mice in this study were between the ages of 8-15 weeks. Wilde-type (WT) C57BL/6 mice were purchased from Kyudo co. *Trem2−/−*, *Card9−/−*, *Clec4e−/−*, *Tyrobp−/−* and *Fcer1g−/−* mice were generated as reported previously27,78,88–90. *Clec4e−/−*, *Tyrobp−/−* and *Fcer1g−/−* mice were kindly provided by Prof. Shizuo Akira (Osaka University), Prof. Toshiyuki Takai (Tohoku University) and Dr. Takashi Saito (RIKEN), respectively. All experiments using mice were approved by the Institutional Animal Research Committee of Kagoshima University and animals were treated in accordance with the ethical guidelines of Kagoshima University.

ITAMR-Fc preparation

Human IgG_1 Fc region was integrated into *Acc*I site of pDisplay (Invitrogen). The ectodomain of Clec2, Mincle, Clec9a, MGL-1, SIGNR1, SIGNR3, DCAR, Clec5a, DC- SIGN (human), TREM1, TREM2, TREM3, LMIR2, LMIR4, LMIR5, LMIR7, LMIR7 and LMIR8 (all from mouse origin except for DC-SIGN) were PCR amplified with the primers in STAR method using cDNA clones (purchased from DNAFORM) as templates, and were inserted into the upstream of the human IgG_1 Fc region in-frame in pDisplay. pDisplay-mouse Dectin-1-Fc (kindly provided by Prof. Naohito Ohno, Tokyo University of Pharmacy and Life Sciences) and pME18S-mouse Dectin-2-Fc79 were used for the following Dectin-1-Fc and Dectin-2-fc expression, respectively . The plasmids were transfected into 293FT cells using Freestyle MAX reagent (Invitrogen) and then cultured according to the manufacturer's instruction. The culture supernatants were collected and then concentrated about 20 times by using VIVASPIN 20 MWCO 30 kDa (Sartorius Stedim). These concentrated supernatants were used in the screening for proteins binding to mycobacteria. For the plate-coated lipid binding assay, TREM2- and Mincle-Fc fusion proteins were purified by using protein G columns as descried previously79.

The 2B4 NFAT-GFP reporter cells

For the construction of DAP12 expression plasmid, SLAM signal sequence-FLAG- mouse DAP12 cassette was PCR amplified from pMX-IRES-GFP-FLAG-DAP12 (kindly provided by Dr. Takashi Saito, RIKEN) with the following primers: 5'- ACGCGTCGACGCCGCCACCATGGATCCCAAAGGATCCCT-3' and 5'-AAGGAAAAAAGCGGCCGCCAGTGTGATGGA-3'. The amplified DNA was then digested with *Sal*I and *Not*I and cloned into *Xho*I and *Not*I sites of pMX-IRES-rCD2 to obtain pMX-IRES-rCD2-FLAG-DAP12. For the construction of TREM1 and TREM2 expression vectors, the coding sequences of mouse TREM1 (amino acids 21-230) and mouse TREM2 (amino acids 19-227) without signal sequences were PCR amplified with the primers: 5'- TACCCATACGATGTTCCAGATTACGCTGCCATTGTTCTAGAG-3' and 5'-AAGGAAAAAAGCCGCTCATCCAAATGTCCT-3'; 5'-TACCCATACGATGTTCCAGATTACGCTCTCAACACCACGGTG-3' and 5'-AAGGAAAAAAGCGGCCGCTCACGTACCTCCGGG-3', respectively. SLAM signal sequence fused with HA was amplified by PCR using the primers: 5'- GAAGATCTGCCGCCACCATGAAAGACGACTTT-3' and 5'-AGCGTAATCTGGAACATCGTATGGGTACACACCTCCACCTGT-3' from pMX-IRES-rCD2-FLAG-DAP12. Then, the SLAM signal sequence-HA cassette was fused to TREM1 or TREM2 PCR products by subsequent PCR amplification and cloned into pMX-IRES-hCD8 to obtain pMX-IRES-hCD8-HA-TREM1 and pMX-IRES-hCD8-HA-TREM2. pMX-rCD2-IRES-FLAG-DAP12 were then retrovirally transfected with or without pMX-IRES-hCD8-HA-TREM1 or pMX-IRES-hCD8-HA-TREM2 into 2B4-NFAT-GFP reporter cells as described previously79. The R47H mutation in TREM2 was generated by KOD –Plus- Mutagenesis Kit (TOYOBO) using pMX-IRES-hCD8-HA- TREM2 as a template. 2B4-NFAT-GFP cells expressing FcRγ and Mincle were generated as descried previously79. For the reporter assay, 5 x 104 reporter cells in 96 well plate were incubated with mycobacteria, soluble PAMPs, or plate-coated lipids for 24 h and then analyzed by Cytoflex flow cytometer (BECKMAN COULTER) and FlowJo software (BD). Percent increase was calculated by dividing GFP MFI values after stimulation by those before stimulation.

Screening for ITAM-coupled receptors binding to mycobacteria

Heat-killed *M. tuberculosis* H37Rv, *M. tuberculosis* H37Ra (Difco) or *M. bovis* BCG were incubated with 20 μg/ml of ITAM receptor-Fc fusion proteins or control Fc fragment protein in RPMI1640 medium for 1 h on ice. After 2 times washing with the medium, the mycobacterial cells were incubated with FITC-conjugated anti-human IgG secondary antibody for 30 min on ice. After a wash, the fluorescence intensity was analyzed by flow cytometer as above. The receptors that showed higher fluorescence intensities than the control values were judged as positive for binding.

Plate-coated lipid binding assay

The lipids (MA, TDM, TDB, PA, THA, GMM, GroMM and HBA) were dissolved in chloroform at 1 mg/ml and then diluted with isopropanol to the working concentrations. Lipid binding assay was performed as described previously91. Briefly, 0.5 μg/well of fMA, GroMM, GMM, and TDM were coated on ELISA plates and then incubated with 0.24 to 1000 nM purified Mincle-Fc or TREM2-Fc proteins in TSM buffer (20 mM Tris–HCl, 150 mM NaCl, 1 mM $CaCl_2$, 2 mM $MgCl_2$, pH 7.0) for 2 h at room temperature. The plates were washed 4 times with 150 μl of TSM buffer , and then incubated with anti- human IgG HRP secondary antibodies for 1 h at room temperature. The binding was detected by colorimetric assay using TMB substrate (Sumitomo Bakelite) and the absorbance at 450 nm was measured by VERSAMax microplate reader (Molecular Devices).

In vitro macrophage stimulation

Peritoneal macrophages were prepared as described previously92. Briefly, 2 ml of 4 % thioglycollate (Difco) solution was intraperitoneally injected into mice. Five days after the injection, peritoneal cells were collected by washing the peritoneum cavity with 5 ml of RPMI 1640 medium containing 10% FCS and 2-mercaptoethanol (RPMI-10). The collected cells were cultured overnight in RPMI-10 and then the adherent cells were used for assays. Bone marrow-derived macrophages (BMDMs) were prepared as described previously 27. Briefly, bone-marrow cells collected from WT, T*rem2−/−*, *Tyrobp−/−* or *Clex4e−/−*mice were cultured in RPMI-10 in the presence of 25 ng of recombinant murine M-CSF (PeproTech) for 3 days, and then the adherent cells were collected as BMDMs. For *in-vitro* cell stimulation, the lipid solutions were added into the 96-well flat bottom plates at 20 μl/well and then the solvent was completely evaporated in a hood before plating macrophages, as described previously30. 1 x 105 cells per well were stimulated with plate-coated lipids or TLR ligands in RPMI-10. The culture supernatants after 24-h culture were collected and the concentrations of TNF (eBioscience), IL-6 (eBioscience), IL-12p40 (Biolegend), IL-10 (Biolegend) and MCP-1 (Biolegend) were analyzed by ELISA kits according to manufacturers' instructions. For Syk inhibition, cells were incubated with 1 μM BAY-613606 (Calbiochem) for 30 min prior to the stimulation.

Measurement of NO production

BMDMs were stimulated in RPMI-10 with 0.1 or 1.0 g per plate of plate-coated MA or TDM in the presence of 10 ng/ml of recombinant IFNγ for 24 h. For the assessment of TNF involvement in NO production, carrier-free recombinant mouse TNF (Biolegend), LEAF purified anti-mouse TNF-α antibody

(MP6-XT22) (BioLegend), or LEAF purified Rat IgG_1 κ Isotype Ctrl antibody (BioLegend) were added to the culture. The culture supernatants were collected and mixed with Griess reagent (1% sulfanilamide, 0.1% *N*- (1-Naphthyl)ethylenediamine dihydrochloride, 2.5% phosphoric acid) at a 1:1 ratio, reacted for 10 min, and the absorbance at 550 nm was measured by a VERSAMax microplate reader. The nitrite concentration was calculated according to the standard curve.

Quantitative real time PCR

Total RNA was isolated from cells using Sepasol-RNA I Super G RNA-isolation kit (Nacalai Tesque). After the removal of DNA contamination by DNase I (Nippon Gene), the total RNA was reverse-transcribed with ReverTra Ace qPCR RT Master Mix (TOYOBO) to synthesize cDNA. Quantitative real-time PCR (qRT-PCR) was performed using THUNDERBIRD SYBR qPCR Mix (TOYOBO) and StepOnePlus (Thermo fisher scientific). The specific primer pairs were “TTGGGTCTTGTTCACTCCACGG” and “CCTCTTTCAGGTCACTTTGGTAGG” for *Nos2* and “AACTTTGGCATTGTGGAAGG” and “ACACATTGGGGGTAGGAACA” for *Gapdh* as an internal control. The relative expression was calculated by ΔΔCt.

MA and TDM emulsions for i.p. administration

Ten mg MA or 2 mg TDM was dissolved in 1 ml of Bayol F (SERVA Electrophoresis) at 64°C, then mixed with 1 ml of PBS using a handy homogenizer (RELIEF). One hundred μl of the emulsion was intraperitoneally injected into WT or *Trem2−/−* mice. The emulsion without lipids was injected as a vehicle control. Peritoneal lavages were collected by washing the peritoneum cavity with RPMI-10. Concentration of cytokine in the lavage was measured by ELISA kit as described above.

TDM emulsion for i.v. administration

TDM emulsion was prepared as described previously30. Briefly, 1 mg of TDM was dissolved in 180 μl of Bayol F at 64°C, then mix with 1.8 ml of 1.1% Tween 80/0.9% NaCl solution to make emulsion. One hundred μl of the emulsion including 50 μg of TDM was intravenously injected into WT and *Trem2−/−* mice. At day 7, the thymuses, lungs, and body weights were measured and the thymus or lung weights were divided by body weights to calculate lung or thymus weight index, respectively. The left lobes were then fixed in 4% paraformaldehyde and embedded in paraffin and stained with hematoxylin and eosin solution. The rest of lung tissues were homogenized by gentleMACS (Miltenyi Biotec) as described previously93 and the concentration of cytokines in homogenates were measured by ELISA kit as described above.

Flow cytometry

For the analysis of infiltrated neutrophils and macrophages, cells in the peritoneal lavage were stained with FITC-conjugated anti-CD11b antibody (M1/70) (eBioscience), PE- conjugated anti-Ly6G antibody (1A8) (eBioscience), and APC-conjugated anti-F4/80 antibody (BM8.1) (TONBO biosciences) after the Fc

blocking with anti-CD16/CD32 antibody (2.4G2) (TONBO biosciences) and analyzed by flow cytometer. For the intracellular iNOS (NOS2) staining, the cells were stained with FITC-conjugated anti- CD11b (M1/70), PE-conjugated anti-F4/80 (Biolegend) and PE-Cy7-conjugated anti- CD38 (90) (Biolegend), and then fixed and permeabilized with BD Cytofix/Cytoperm kits (BD Biosciences). After washing, the cells were stained with APC-conjugated anti-NOS2 antibody (CXNFT) (eBioscience) and analyzed by flow cytometer.

M. bovis BCG infection

I*n-vitro* infection of *M. bovis* BCG was performed as described previously94. Briefly, BMDMs (1 x 105) from WT of *Trem2−/−* mice were and infected in 96-well plate with 1 x 106 (MOI 10:1) of live *M. bovis* BCG (Tokyo 172 strain, Japan BCG laboratory) for 4h. After the infection, uninfected bacteria were washed-out with RPMI-10 and the infected cells were further cultured for 24 h in RPMI-10. The supernatant was collected and he nitrite concentration was measured by Griess assay. The cells were disrupted by water and plated on Middlebrook 7H10 agar (Difco) and number of BCG colonies was counted after 3 week culture for CFU determination. I*n vivo* infection was performed as described previously95. WT and *Trem2−/−* mice were infected intraperitoneally with 5.0 x 106 CFU of live *M. bovis* BCG. The peritoneal lavages were collected at indicated time point by washing the peritoneal cavity with 1 ml of RPMI-10. The concentration of cytokines in the lavage was analyzed by ELISA kit as described above. The recruited peritoneal cells were analyzed by flow cytometer as described above. For CFU counting, the peritoneal cells were disrupted by water and plated on Middlebrook 7H10 agar and colonies were counted as described above.

Statistical analysis

All statistical analyses were carried out using Prism 5 software. Student's *t*-test was performed for the comparisons between TDM and fMA in Fig. 5I-K or between WT and *Trem2−/−* mice in Fig. 7A, B. One-way ANOVA or two-way ANOVA with Bonferroni post hoc test were performed for the comparison of multiple groups. *P* values <0.05 were considered statistically significant.

Declarations

ACKNOWLEDGMENTS

We thank Dr. Fumika Mi-ichi for discussion and helpful suggestions; Ryoko Muroya and Shizuko Furukawa for secretarial assistance; Emi Kirino, Ritsuko Yoshia, and Shoko Takao for technical assistance. This work was supported by Grant-in-Aid for Scientific Research 15H04729 (H.H.) and for Young Scientists 26860292 (E.I.), the Foundation for Research Fellowships of JSPS for Young Scientists (PD) Grant 23-2866 (E.I.), GSK Japan Research Grant 2015 (E.I.), The Uehara Memorial Foundation (H.H.), Takeda Science Foundation (H.H.), The NOVARTIS Foundation (Japan) for the Promotion of Science (H.H.), The Naito Foundation (H.H.), and the Kodama Memorial Fund for Medical Research (H.H. and E.I.).

AUTHOR CONTRIBUTIONS

E.I. and H.H. designed the research; E.I., Y.C., M.U., M.K., H.K., H.K., and K.T. performed the experiments and analyzed the data; S.Y., M.C., and M.S. provided materials; E.I., M.U., M.K., H.K., I.Y., T.U., G.M., S.Y., H.Y., and H.H. discussed the data; E.I. and H.H. wrote the manuscript; H.H. supervised the research.

COMPETING INTERESTS STATEMENT

The authors declare no competing interests.

References

1. Peddireddy, V., Doddam, S. N. & Ahmed, N. Mycobacterial Dormancy Systems and Host Responses in Tuberculosis. *Front. Immunol.* **8**, (2017).
2. Brennan, P. J. Structure, function, and biogenesis of the cell wall of Mycobacterium tuberculosis. *Tuberculosis* **83**, 91–97 (2003).
3. Dulberger, C. L., Rubin, E. & Boutte, C. C. The mycobacterial cell envelope - a moving target. *Nat. Rev. Microbiol.* **18**, 47–59 (2020).
4. Queiroz, A., Riley, W., Queiroz, A. & Riley, L. W. Bacterial immunostat: Mycobacterium tuberculosis lipids and their role in the host immune response. *Rev. Soc. Bras. Med. Trop.* **50**, 9–18 (2017).
5. Marrakchi, H., Lanéelle, M.-A. & Daffé, M. Mycolic Acids: Structures, Biosynthesis, and Beyond. *Chem. Biol.* **21**, 67–85 (2014).
6. Bacon, *et al.* Non-Replicating Mycobacterium tuberculosis Elicits a ReducedInfectivity Profile with Corresponding Modifications to the Cell Wall and Extracellular Matrix. *PLoS ONE* **9**, (2014).
7. Matsunaga, I. *et al.* Mycolyltransferase-mediated Glycolipid Exchange in Mycobacteria. *J. Biol. Chem.* **283**, 28835–28841 (2008).
8. Kaneda, K., Sumi, , Kurano, F., Kato, Y. & Yano, I. Granuloma formation and hemopoiesis induced by C36-48-mycolic acid-containing glycolipids from Nocardia rubra. *Infect. Immun.* **54**, 869–875 (1986).
9. Sarmiento, M. E. *et al.* Tuberculosis vaccine candidates based on mycobacterial cell envelope components. *Tuberculosis* **115**, 26–41 (2019).
10. Ojha, A. K. *et al.* Growth of Mycobacterium tuberculosis biofilms containing free mycolic acids and harbouring drug-tolerant bacteria. *Microbiol.* **69**, 164–174 (2008).
11. Ojha, A. K., Trivelli, , Guerardel, Y., Kremer, L. & Hatfull, G. F. Enzymatic Hydrolysis of Trehalose Dimycolate Releases Free Mycolic Acids during Mycobacterial Growth in Biofilms. *J. Biol. Chem.* **285**, 17380–17389 (2010).

12. Cantrell, A. *et al.* Free mycolic acid accumulation in the cell wall of the mce1 operon mutant strain of Mycobacterium tuberculosis. *J. Microbiol.* **51**, 619–626 (2013).

13. Shimono, N. *et al.* Hypervirulent mutant of Mycobacterium tuberculosis resulting from disruption of the mce1 *Proc. Natl. Acad. Sci.* **100**, 15918–15923 (2003).

14. Sequeira, C., Senaratne, R. H. & Riley, L. W. Inhibition of toll-like receptor 2 (TLR- 2)-mediated response in human alveolar epithelial cells by mycolic acids and Mycobacterium tuberculosis mce1 operon mutant. *Pathog. Dis.* **70**, 132–140 (2014).

15. Layre, E. *et al.* Mycolic Acids Constitute a Scaffold for Mycobacterial Lipid Antigens Stimulating CD1-Restricted T Cells. *Biol.* **16**, 82–92 (2009).

16. Hattori, Y. *et al.* Glycerol monomycolate, a latent tuberculosis-associated mycobacterial lipid, induces eosinophilic hypersensitivity responses in guinea pigs. *Biochem. Biophys. Res. Commun.* **409**, 304–307 (2011).

17. Price, V. & Vance, R. E. The Macrophage Paradox. *Immunity* **41**, 685–693 (2014).

18. Boggiano, C. *et al.* "The Impact of Mycobacterium tuberculosis Immune Evasion on Protective Immunity: Implications for TB Vaccine Design" – Meeting *Vaccine* **35**, 3433–3440 (2017).

19. Reed, M. B. *et al.* A glycolipid of hypervirulent tuberculosis strains that inhibits the innate immune response. *Nature* **431**, 84–87 (2004).

20. Cambier, J. *et al.* Mycobacteria manipulate macrophage recruitment through coordinated use of membrane lipids. *Nature* **505**, 218–222 (2013).

21. Cambier, J., O'Leary, S. M., O'Sullivan, M. P., Keane, J. & Ramakrishnan, L. Phenolic Glycolipid Facilitates Mycobacterial Escape from Microbicidal Tissue- Resident Macrophages. *Immunity* **47**, 552-565.e4 (2017).

22. Ford, W. & McVicar, D. W. TREM and TREM-like receptors in inflammation and disease. *Curr. Opin. Immunol.* **21**, 38–46 (2009).

23. Hardison, S. E. & Brown, G. D. C-type lectin receptors orchestrate antifungal *Nat. Immunol.* **13**, 817–822 (2012).

24. Ivashkiv, B. Cross-regulation of signaling by ITAM-associated receptors. *Nat. Immunol.* **10**, 340–347 (2009).

25. Osorio, F. & Reis e Sousa, C. Myeloid C-type Lectin Receptors in Pathogen Recognition and Host Defense. *Immunity* **34**, 651–664 (2011).

26. Hara, H. *et al.* Cell Type-Specific Regulation of ITAM-Mediated NF-κB Activation by the Adaptors, CARMA1 and CARD9. *J. Immunol.* **181**, 918–930 (2008).

27. Hara, H. *et al.* The adaptor protein CARD9 is essential for the activation of myeloid cells through ITAM-associated and Toll-like *Nat Immunol* **8**, 619–629 (2007).

28. Ishikawa, E., Mori, D. & Yamasaki, Recognition of Mycobacterial Lipids by Immune Receptors. *Trends Immunol.* **38**, 66–76 (2017).
29. Dorhoi, A. *et al.* The adaptor molecule CARD9 is essential for tuberculosis control. *J. Exp. Med.* **207**, 777–792 (2010).
30. Ishikawa, E. *et al.* Direct recognition of the mycobacterial glycolipid, trehalose dimycolate, by C-type lectin Mincle. *Exp. Med.* **206**, 2879–2888 (2009).
31. Miyake, Y. *et al.* C-type Lectin MCL Is an FcRγ-Coupled Receptor that Mediates the Adjuvanticity of Mycobacterial Cord Factor. *Immunity* **38**, 1050–1062 (2013).
32. Miyake, Y. , Oh-hora, M. & Yamasaki, S. C-Type Lectin Receptor MCL Facilitates Mincle Expression and Signaling through Complex Formation. *J. Immunol.* **194**, 5366–5374 (2015).
33. Yonekawa, A. *et al.* Dectin-2 Is a Direct Receptor for Mannose-Capped Lipoarabinomannan of Mycobacteria. *Immunity* **41**, 402–413 (2014).
34. Toyonaga, K. *et al.* C-Type Lectin Receptor DCAR Recognizes Mycobacterial Phosphatidyl-Inositol Mannosides to Promote a Th1 Response during Infection. *Immunity* **45**, 1245–1257 (2016).
35. Divangahi, M. *et al.* Critical Negative Regulation of Type 1 T Cell Immunity and Immunopathology by Signaling Adaptor DAP12 during Intracellular Infection. *J. Immunol.* **179**, 4015–4026 (2007).
36. Jeyanathan, M. *et al.* Pulmonary M. tuberculosis infection delays Th1 immunity via immunoadaptor DAP12-regulated IRAK-M and IL-10 expression in antigen- presenting cells. *Mucosal Immunol.* **7**, 670–683 (2014).
37. Borrego, F. The CD300 molecules: an emerging family of regulators of the immune system. *Blood* **121**, 1951–1960 (2013).
38. Dambuza, I. M. & Brown, G. D. C-type lectins in immunity: recent *Curr. Opin. Immunol.* **32**, 21–27 (2015).
39. Park, C. G. *et al.* Five mouse homologues of the human dendritic cell C-type lectin, DC-SIGN. *Immunol.* **13**, 1283–1290 (2001).
40. Koppel, E. A. *et al.* Identification of the mycobacterial carbohydrate structure that binds the C-type lectins DC-SIGN, L-SIGN and SIGNR1. *Immunobiology* **209**, 117– 127 (2004).
41. Bouchon, A., Hernández-Munain, C., Cella, M. & Colonna, M. A Dap12-Mediated Pathway Regulates Expression of Cc Chemokine Receptor 7 and Maturation of Human Dendritic *J. Exp. Med.* **194**, 1111–1122 (2001).
42. Peng, Q. *et al.* TREM2- and DAP12-Dependent Activation of PI3K Requires DAP10 and Is Inhibited by SHIP1. *Sci Signal* **3**, ra38 (2010).
43. Ghazaei, C. Mycobacterium tuberculosis and lipids: Insights into molecular mechanisms from persistence to virulence. *Res. Med. Sci. Off. J. Isfahan Univ. Med. Sci.* **23**, (2018).

44. Cannon, P., O'Driscoll, M. & Litman, G. W. Specific lipid recognition is a general feature of CD300 and TREM molecules. *Immunogenetics* **64**, 39–47 (2012).
45. Wang, Y. *et al.* TREM2 Lipid Sensing Sustains the Microglial Response in an Alzheimer's Disease Model. *Cell* **160**, 1061–1071 (2015).
46. Cady, J. *et al.* TREM2 Variant p.R47H as a Risk Factor for Sporadic Amyotrophic Lateral Sclerosis. *JAMA Neurol.* **71**, 449–453 (2014).
47. Guerreiro, R. *et al.* TREM2 Variants in Alzheimer's Disease. *N. Engl. J. Med.* **368**, 117–127 (2013).
48. Jonsson, T. *et al.* Variant of TREM2 Associated with the Risk of Alzheimer's Disease. N. *Engl. J. Med.* **368**, 107–116 (2013).
49. Singaraja, R. TREM2: a new risk factor for Alzheimer's disease. *Clin. Genet.* **83**, 525– 526 (2013).
50. Kober, L. *et al.* Neurodegenerative disease mutations in TREM2 reveal a functional surface and distinct loss-of-function mechanisms. *eLife* **5**, e20391 (2016).
51. Verschoor, A., Baird, M. S. & Grooten, J. Towards understanding the functional diversity of cell wall mycolic acids of Mycobacterium tuberculosis. *Prog. Lipid Res.* **51**, 325–339 (2012).
52. Deshmane, L., Kremlev, S., Amini, S. & Sawaya, B. E. Monocyte Chemoattractant Protein-1 (MCP-1): An Overview. *J. Interferon Cytokine Res.* **29**, 313–326 (2009).
53. Kipnis, A., Basaraba, R. J., Orme, I. M. & Cooper, A. M. Role of chemokine ligand 2 in the protective response to early murine pulmonary tuberculosis. *Immunology* **109**, 547–551 (2003).
54. Peters, W. *et al.* Chemokine receptor 2 serves an early and essential role in resistance to Mycobacterium tuberculosis. *Proc. Natl. Acad. Sci.* **98**, 7958–7963 (2001).
55. Bean, A. G. D. *et al.* Structural Deficiencies in Granuloma Formation in TNF Gene- Targeted Mice Underlie the Heightened Susceptibility to Aerosol Mycobacterium tuberculosis Infection, Which Is Not Compensated for by *J. Immunol.* **162**, 3504–3511 (1999).
56. Harris, J. & Keane, J. How tumour necrosis factor blockers interfere with tuberculosis immunity. *Clin. Exp. Immunol.* **161**, 1–9 (2010).
57. Hara, H. & Saito, T. CARD9 versus CARMA1 in innate and adaptive immunity. *Trends Immunol.* **30**, 234–242 (2009).
58. Werninghaus, K. *et al.* Adjuvanticity of a synthetic cord factor analogue for subunit Mycobacterium tuberculosis vaccination requires FcRγ–Syk–Card9–dependent innate immune activation. *Exp. Med.* **206**, 89–97 (2009).
59. MacMicking, D. *et al.* Identification of nitric oxide synthase as a protective locus against tuberculosis. *Proc. Natl. Acad. Sci.* **94**, 5243–5248 (1997).
60. Weiss, G. & Schaible, U. E. Macrophage defense mechanisms against intracellular bacteria. *Immunol. Rev.* **264**, 182–203 (2015).

61. Lee, M. *et al.* Minocycline inhibits apoptotic cell death via attenuation of TNF-α expression following iNOS/NO induction by lipopolysaccharide in neuron/glia co- cultures. *J. Neurochem.* **91**, 568–578 (2004).

62. Seo, W.-G. *et al.* Synergistic cooperation between water-soluble chitosan oligomers and interferon-γ for induction of nitric oxide synthesis and tumoricidal activity in murine peritoneal macrophages. *Cancer Lett.* **159**, 189–195 (2000).

63. Sol, V., Díaz-Muñoz, M. D. & Fresno, M. Requirement of tumor necrosis factor α and nuclear factor-κB in the induction by IFN-γ of inducible nitric oxide synthase in macrophages. *J. Leukoc. Biol.* **81**, 272–283 (2007).

64. Jablonski, K. A. *et al.* Novel Markers to Delineate Murine M1 and M2 *PLOS ONE* **10**, e0145342 (2015).

65. Cambier, J., Falkow, S. & Ramakrishnan, L. Host Evasion and Exploitation Schemes of Mycobacterium tuberculosis. *Cell* **159**, 1497–1509 (2014).

66. Sharif, O. & Knapp, S. From expression to signaling: Roles of TREM-1 and TREM-2 in innate immunity and bacterial infection. *Immunobiology* **213**, 701–713 (2008).

67. Paloneva, J. *et al.* Loss-of-function mutations in TYROBP (DAP12) result in a presenile dementia with bone cysts. *Nat. Genet.* **25**, 357–361 (2000).

68. Paloneva, J. *et al.* Mutations in Two Genes Encoding Different Subunits of a Receptor Signaling Complex Result in an Identical Disease Phenotype. *Am. J. Hum. Genet.* **71**, 656–662 (2002).

69. Daws, R. *et al.* Pattern Recognition by TREM-2: Binding of Anionic Ligands. *J. Immunol.* **171**, 594–599 (2003).

70. Stefano, L. *et al.* The surface-exposed chaperone, Hsp60, is an agonist of the microglial TREM2 receptor. *Neurochem.* **110**, 284–294 (2009).

71. Quan, D. N. *et al.* TREM-2 binds to lipooligosaccharides of Neisseria gonorrhoeae and is expressed on reproductive tract epithelial *Mucosal Immunol.* **1**, 229–238 (2008).

72. Yeh, L., Wang, Y., Tom, I., Gonzalez, L. C. & Sheng, M. TREM2 Binds to Apolipoproteins, Including APOE and CLU/APOJ, and Thereby Facilitates Uptake of Amyloid-Beta by Microglia. *Neuron* **91**, 328–340 (2016).

73. Hattori, Y. *et al.* Glycerol Monomycolate Is a Novel Ligand for the Human, but Not Mouse Macrophage Inducible C-type Lectin, Mincle. *J. Biol. Chem.* **289**, 15405– 15412 (2014).

74. Hasan, Z. *et al.* CCL2 Responses to Mycobacterium tuberculosis Are Associated with Disease Severity in Tuberculosis. *PLoS ONE* **4**, e8459 (2009).

75. Feng, W.-X. *et al.* CCL2–2518 (A/G) polymorphisms and tuberculosis susceptibility: a meta-analysis [Review article]. *Int. J. Tuberc. Lung Dis.* **16**, 150–156 (2012).

76. Flores-Villanueva, O. *et al.* A functional promoter polymorphism in monocyte chemoattractant protein–1 is associated with increased susceptibility to pulmonary tuberculosis. *J. Exp. Med.* **202**, 1649–1658 (2005).
77. Yu, J. *et al.* Both Phthiocerol Dimycocerosates and Phenolic Glycolipids Are Required for Virulence of Mycobacterium marinum. *Infect. Immun.* **80**, 1381–1389 (2012).
78. Ito, H. & Hamerman, J. A. TREM-2, triggering receptor expressed on myeloid cell- 2, negatively regulates TLR responses in dendritic cells. *Eur. J. Immunol.* doi:10.1002/eji.201141679.
79. Turnbull, I. R. *et al.* Cutting edge: TREM-2 attenuates macrophage activation. *Immunol. Baltim. Md 1950* **177**, 3520–3524 (2006).
80. Yamasaki, S. *et al.* Mincle is an ITAM-coupled activating receptor that senses damaged cells. *Nat Immunol* **9**, 1179–1188 (2008).
81. Nagata, M. *et al.* Intracellular metabolite β-glucosylceramide is an endogenous Mincle ligand possessing immunostimulatory *Proc. Natl. Acad. Sci.* **114**, E3285–E3294 (2017).
82. Lee, W.-B. *et al.* Mincle-mediated translational regulation is required for strong nitric oxide production and inflammation resolution. *Nat. Commun.* **7**, 1–14 (2016).
83. Ryll, R., Kumazawa, Y. & Yano, I. Immunological Properties of Trehalose Dimycolate (Cord Factor) and Other Mycotic Acid-Containing Glycolipids–-A Review. *Microbiol. Immunol.* **45**, 801–811 (2001).
84. Takahashi, K., Rochford, C. D. & Neumann, H. Clearance of apoptotic neurons without inflammation by microglial triggering receptor expressed on myeloid cells- 2. *J. Exp. Med.* **201**, 647–657 (2005).
85. Takahashi, K., Prinz, M., Stagi, M., Chechneva, O. & Neumann, H. TREM2-Transduced Myeloid Precursors Mediate Nervous Tissue Debris Clearance and Facilitate Recovery in an Animal Model of Multiple Sclerosis. *PLoS Med* **4**, e124 (2007).
86. Hsieh, L. *et al.* A role for TREM2 ligands in the phagocytosis of apoptotic neuronal cells by microglia. *J. Neurochem.* **109**, 1144–1156 (2009).
87. Sica, A. & Mantovani, A. Macrophage plasticity and polarization: in vivo veritas. *J. Clin. Invest.* **122**, 787–795 (2012).
88. Seno, H. *et al.* Efficient colonic mucosal wound repair requires Trem2 signaling. *Proc. Natl. Acad. Sci.* **106**, 256–261 (2009).
89. Kaifu, T. *et al.* Osteopetrosis and thalamic hypomyelinosis with synaptic degeneration in DAP12-deficient mice. *J. Clin. Invest.* **111**, 323–332 (2003).
90. Park, Y. *et al.* Resistance of Fc receptor- deficient mice to fatal glomerulonephritis. *J. Clin. Invest.* **102**, 1229–1238 (1998).
91. Yamasaki, S. *et al.* C-type lectin Mincle is an activating receptor for pathogenic fungus, Malassezia. *Proc. Natl. Acad. Sci.* **106**, 1897–1902 (2009).

92. Phongsisay, V., Iizasa, E., Hara, H. & Yamasaki, S. LMIR5 extracellular domain activates myeloid cells through Toll-like receptor 4. *Mol. Immunol.* **62**, 169–177 (2014).
93. Saijo, S. *et al.* Dectin-1 is required for host defense against Pneumocystis carinii but not against Candida albicans. *Nat. Immunol.* **8**, 39–46 (2007).
94. Van Dyken, S. *et al.* Chitin Activates Parallel Immune Modules that Direct Distinct Inflammatory Responses via Innate Lymphoid Type 2 and γδ T Cells. *Immunity* **40**, 414–424 (2014).
95. Shin, D.-M. *et al.* Mycobacterium tuberculosis Eis Regulates Autophagy, Inflammation, and Cell Death through Redox-dependent *PLOS Pathog.* **6**, e1001230 (2010).
96. Nau, G. *et al.* Attenuated Host Resistance againstMycobacterium bovis BCG Infection in Mice Lacking Osteopontin. *Infect. Immun.* **67**, 4223–4230 (1999).

Figures

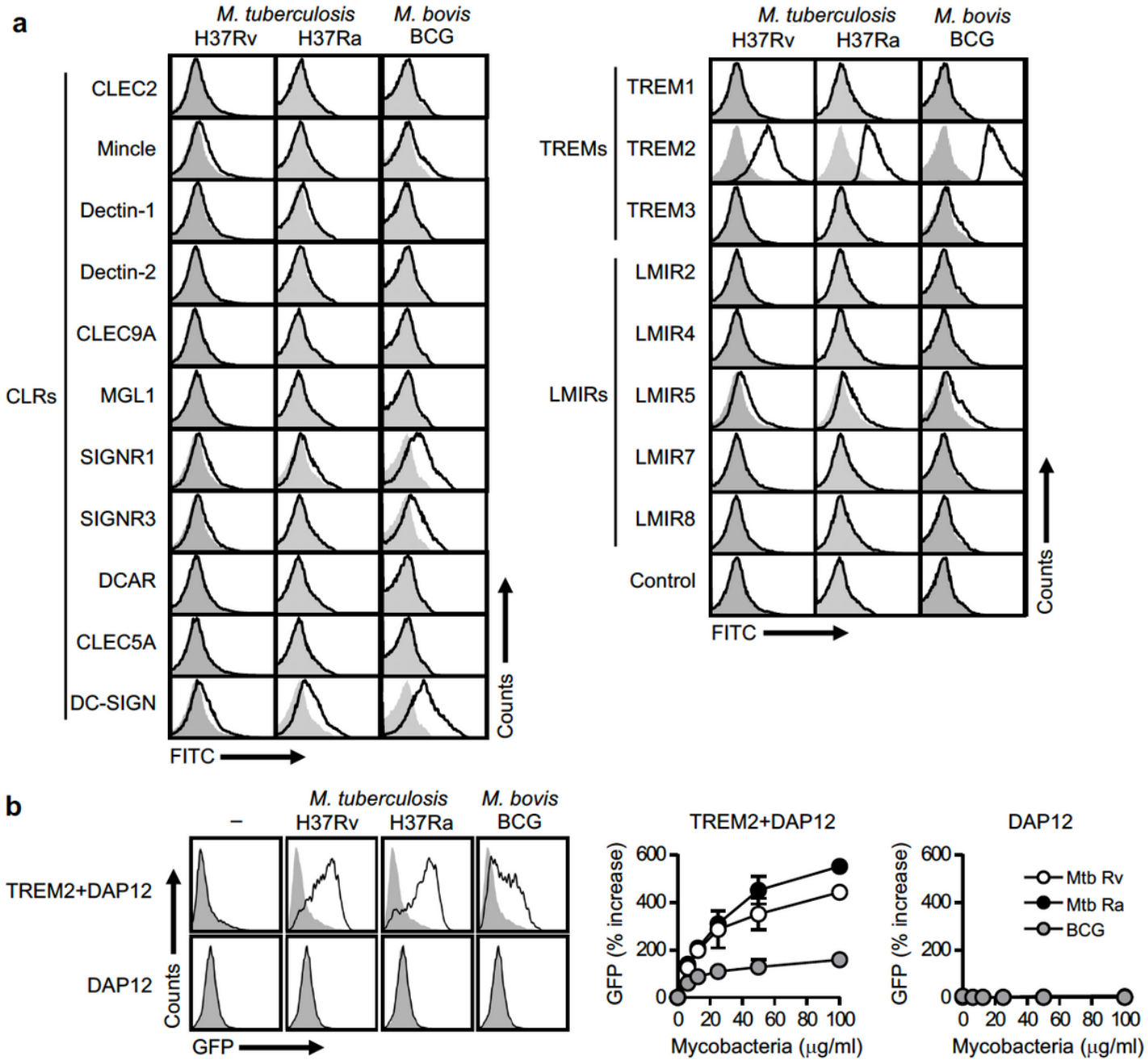

Figure 1

TREM2 recognizes mycobacteria. (a) Heat-killed Mtb H37Ra or H37Rv, or M. bovis BCG were incubated with the indicated CLR, TREM and LMIR family receptors fused to the Fc antibody fragment or with the control Fc fragment, followed by staining with anti-human IgG-FITC secondary antibody. The binding of each receptor-Fc protein was analyzed by flow cytometry. Open histograms show binding data for the indicated receptor-Fc proteins. The gray-filled histograms show background fluorescence of the control staining. (b) NFAT-GFP reporter cells expressing TREM2+DAP12 or DAP12 alone were stimulated with the indicated amounts of heat-killed Mtb H37Ra or H37Rv, or M. bovis BCG for 24 h, followed by analysis of GFP fluorescence by flow cytometry. The histograms on the left indicate the data from stimulation with

100 μg/ml of the indicated mycobacteria. Data in the right panels are presented as percent increase over control values of unstimulated cells. Data are presented as the mean ± SEM of duplicate assays and representative of three independent experiments.

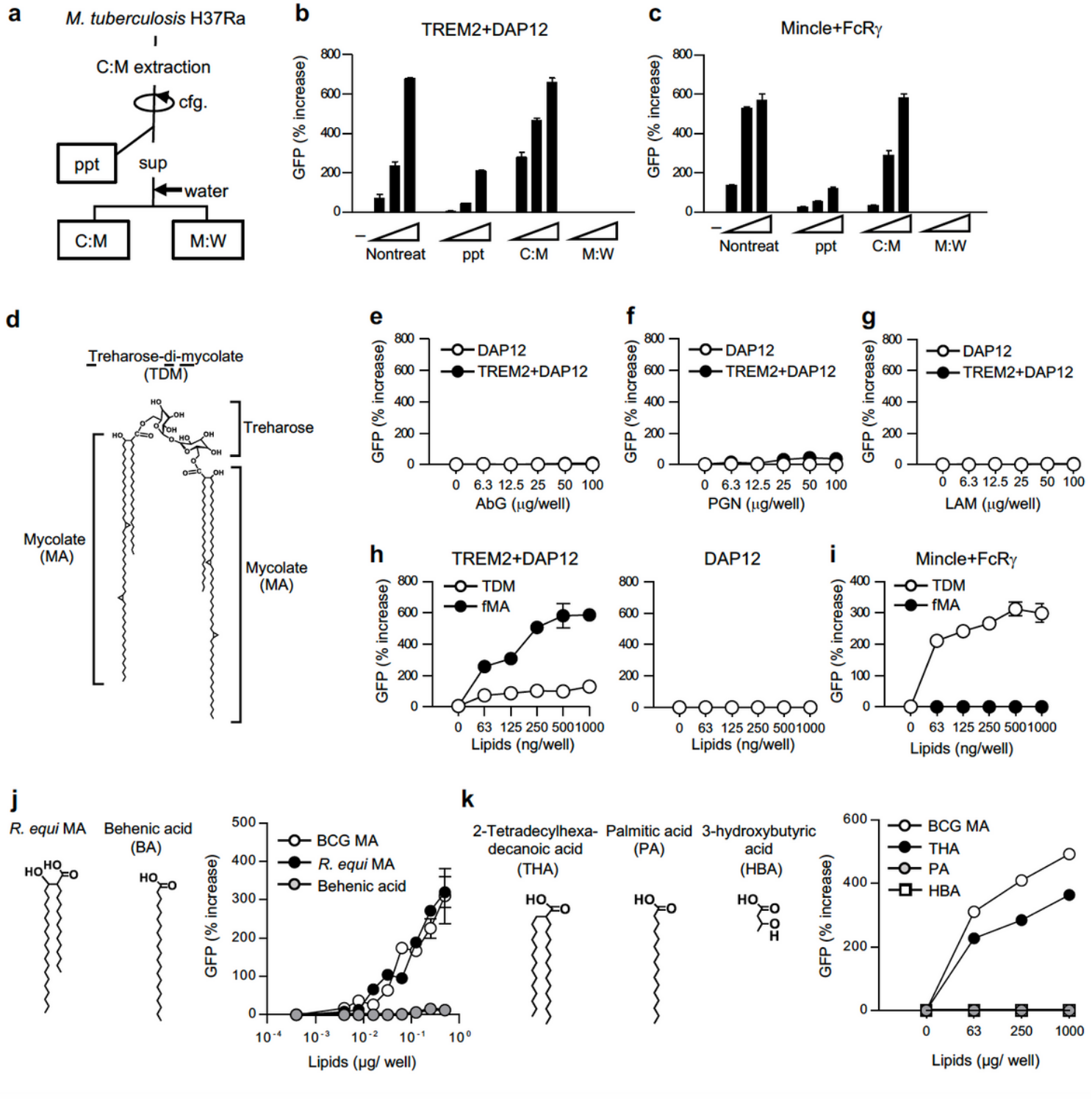

Figure 2

TREM2 recognizes MAs. (a) Schematic diagram of solvent-based de-lipidation and fractionation of Mtb H37Ra. Bacteria were de-lipidated by treatment with C:M. After centrifugation (cfg.), soluble extracts (sup)

were mixed with water and separated into the lipid-soluble (C:M) and the water-soluble methanol:water (M:W) fractions. (b, c) NFAT- GFP-reporter cells expressing TREM2+DAP12 (b) or Mincle+FcRγ (c) were stimulated for 24 h with either untreated or de-lipidated bacteria (ppt) or plate-coated C:M or M:W fractions indicated in (a), followed by analysis of GFP fluorescence by flow cytometry. (d) Chemical structure of TDM. The structure of α -mycolate containing TDM is shown. (e–g) NFAT-GFP-reporter cells expressing TREM2+DAP12 or DAP12 alone were stimulated with the indicated amounts of ABG (e), PGN (f), and LAM (g) for 24 h, followed by analysis of GFP fluorescence by flow cytometry. Data are presented as percent increase over control values of unstimulated cells. (h, i) NFAT-GFP-reporter cells expressing TREM2+DAP12 or DAP12 only (h) or Mincle+FcRγ (i) were stimulated with the indicated amounts of TDM or fMA and analyzed as described in (e–g). (j, k) NFAT- GFP-reporter cells expressing TREM2+DAP12 were stimulated with the indicated amounts of BCG MA, R. equi MA, or BA (j) or THA, PA, or HBA (k) and analyzed as described in (e-g).

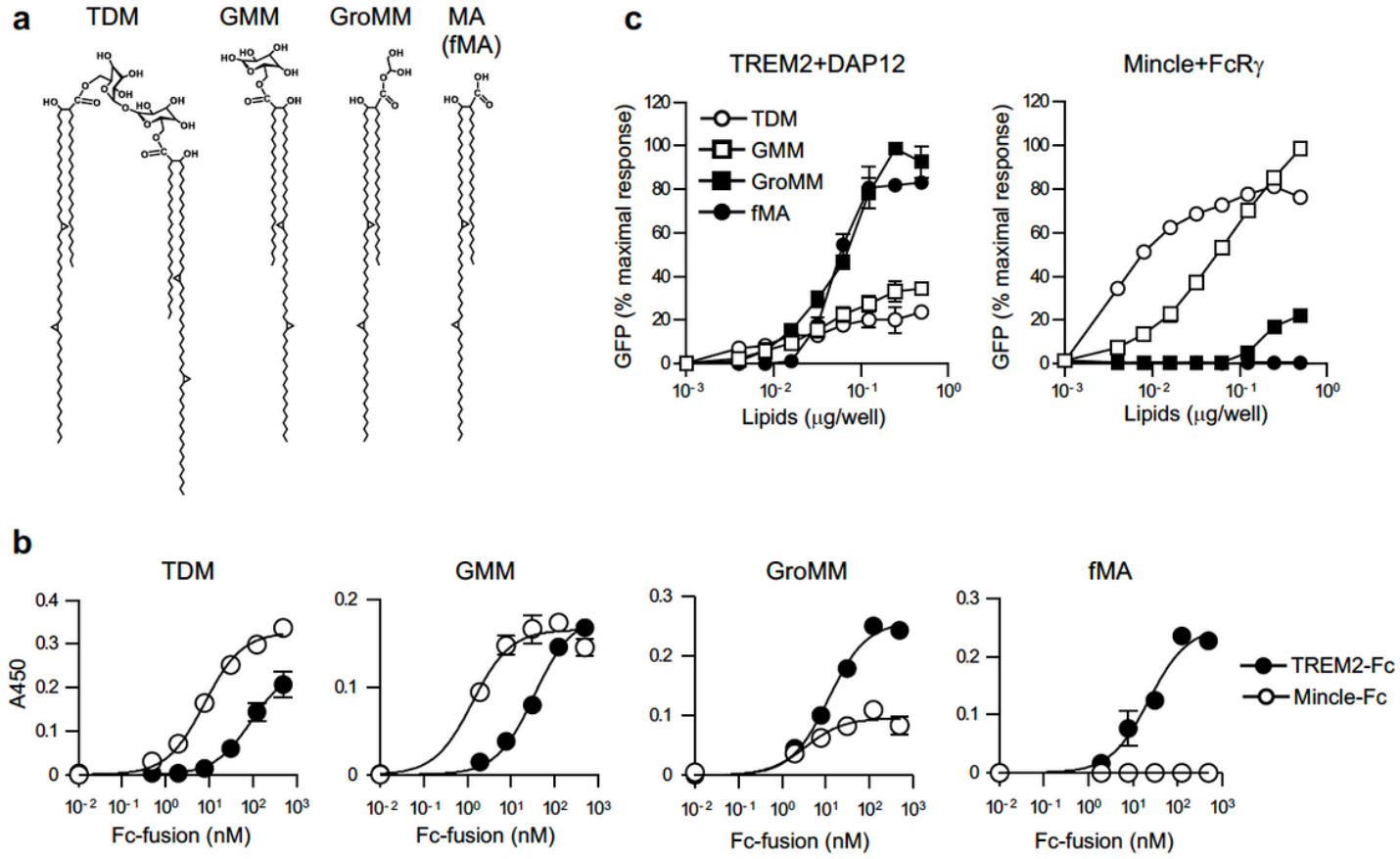

Figure 3

TREM2 and Mincle preferentially recognize distinct MA-containing lipids based on their glycosylation. (a) Chemical structure of glycosylated (TDM and GMM) and non- glycosylated (GroMM and fMA) MA-containing lipids found in Mtb. The structures of α-mycolate-containing lipids are included. (b) The indicated amounts of TREM2 or Mincle-Fc fusion proteins were added to wells coated with 0.5 μg/well TDM, GMM, GroMM, or fMA, followed by incubation with anti-human IgG-horseradish peroxidase and

detection of bound proteins using an enzyme-linked immunosorbent assay (ELISA)- based colorimetric assay. (c) NFAT-GFP-reporter cells expressing TREM2+DAP12 or Mincle+FcRγ were stimulated with the indicated amounts of TDM, GMM, GroMM, or fMA coated on the plates for 24 h, followed by analysis of GFP fluorescence by flow cytometry. Values are plotted as percent maximal response of the largest value. Data are presented as mean ± SEM of triplicate assays and are representative of at least three independent experiments.

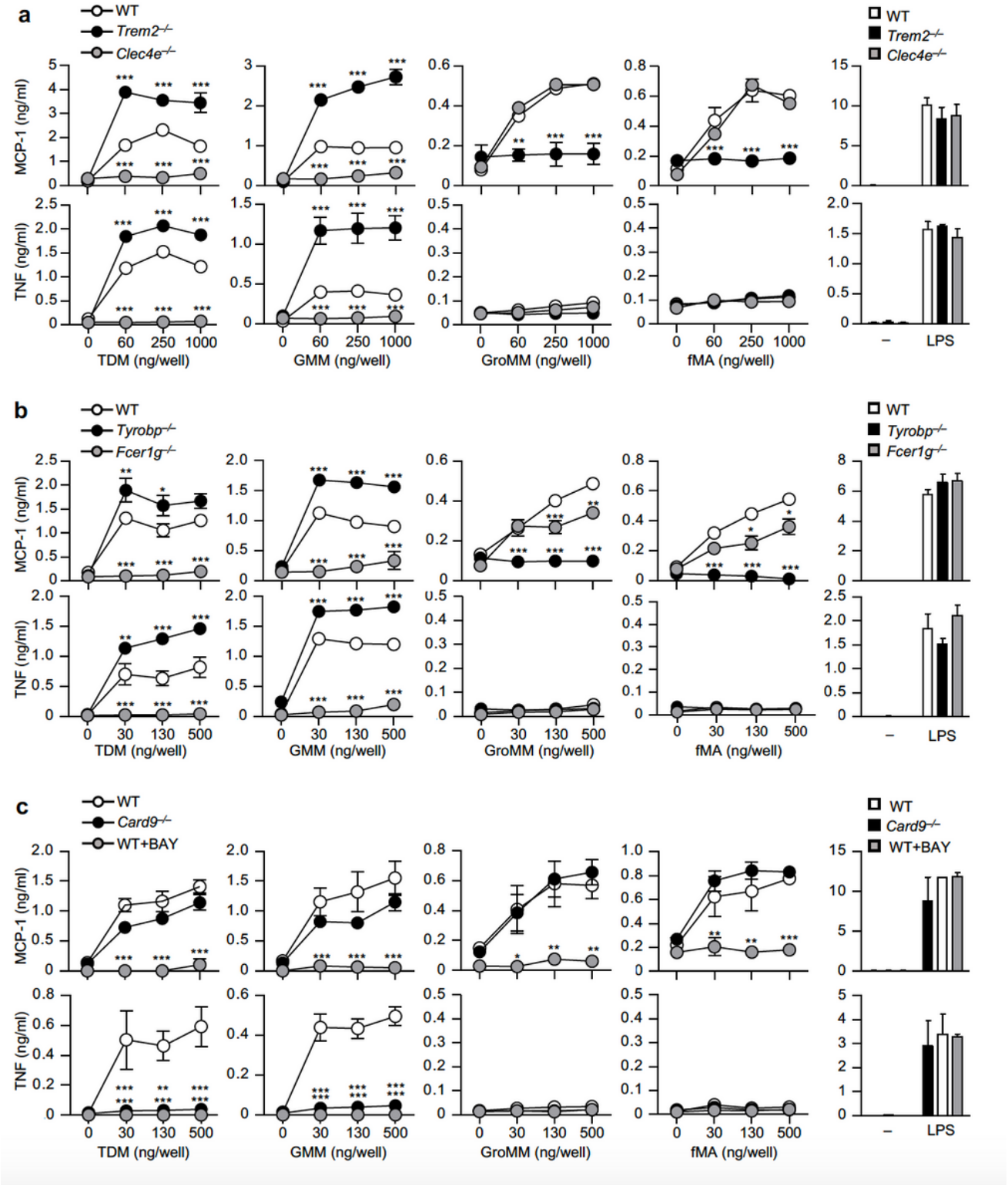

Figure 4

Glycosylated and non-glycosylated MAs elicit distinct macrophage activation through Mincle and TREM2, respectively. (a–c) Peritoneal macrophages from wild-type (WT), Trem2–/–, or Clec4e–/– mice (a), WT, Tyrobp–/–, or Fcer1g–/– mice (b), or WT or Card9–/– mice (c) were stimulated with the indicated amounts of TDM, GMM, GroMM, or fMA coated on the plates or with LPS (100 ng/ml) for 24 h. WT cells were stimulated in the presence or absence of the Syk inhibitor BAY-613606 (BAY) (c). MCP-1 and TNF production in the culture supernatant was measured by ELISA. Data are presented as the mean ± SEM of triplicate assays and are representative of three independent experiments. *$p < 0.05$, **$p < 0.01$, ***$p < 0.001$.

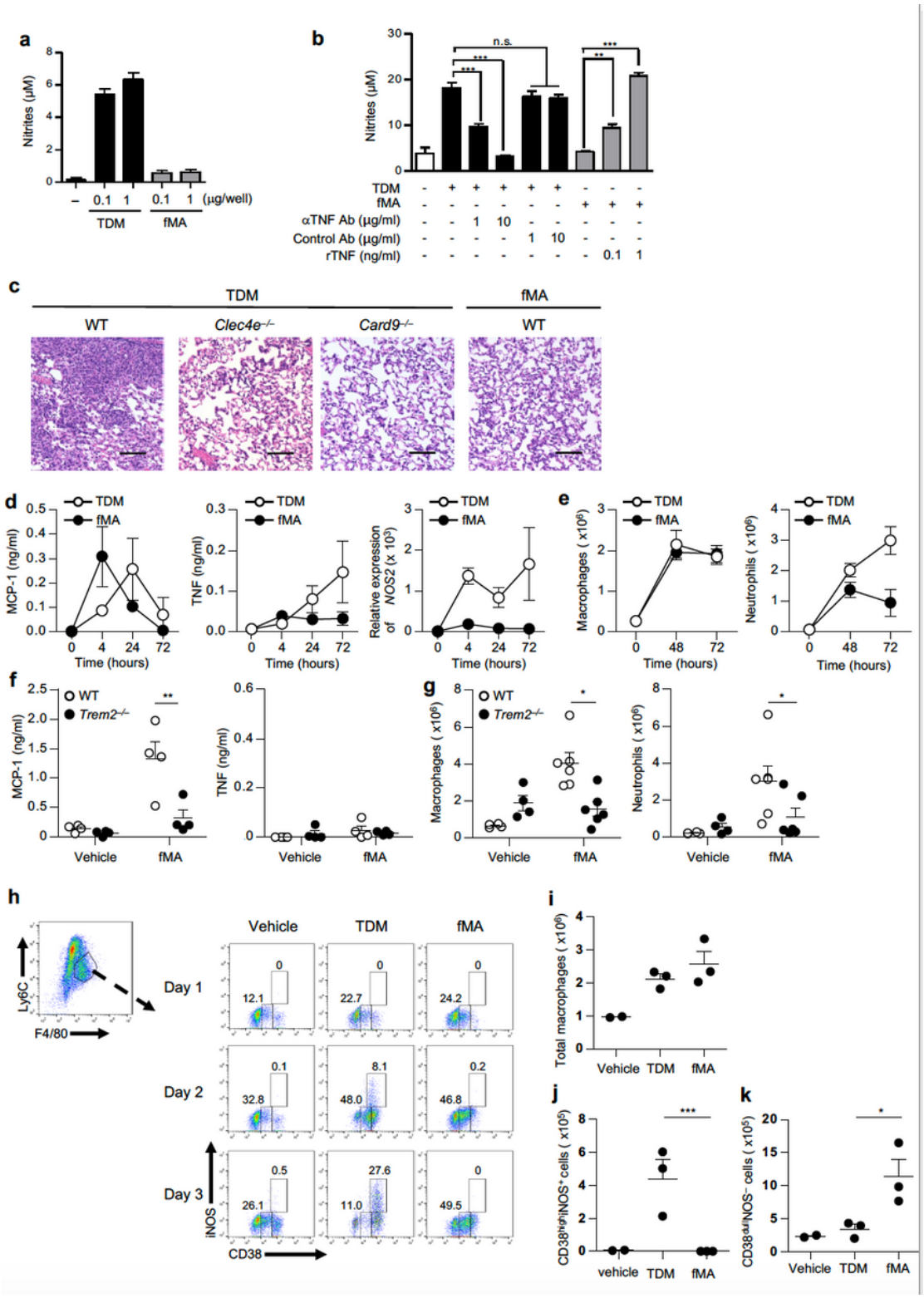

Figure 5

Triggering of TREM2 by MA induces the permissive macrophages. (a, b) BMDMs were stimulated for 24 h with the indicated amount of TDM or fMA coated on the plates in the presence of 10 ng/ml IFNγ (a), stimulated with 1 μg of TDM coated on the plates with or without the indicated amounts of a TNF-blocking antibody (αTNF Ab) or an isotype-matched control antibody (Control Ab) (b), or stimulated with 1 μg of fMA coated on the plates with or without recombinant TNF (rTNF) (b). NO production was

determined by measuring nitrite concentration in the culture supernatants by Griess assay. Data are presented as the mean ± SEM of triplicate assays and are representative of three independent experiments. **p < 0.01, ***p < 0.001. (c) Representative images of the hematoxylin & eosin-stained lungs from WT, Clec4e−/−, or Card9−/− mice at day 7 after intravenous injection of 50 μg TDM or 250 μg fMA emulsion. Control mice did not exhibit any inflammatory manifestations in the lungs after receiving the control (vehicle) emulsion injection. Scale bars: 0.1 mm. (d–f) WT mice (n = 4) were injected intraperitoneally with 500 μg fMA or 100 μg TDM emulsion, and peritoneal lavages were collected at 4-, 24-, and 72-h post-injection. MCP-1 and TNF concentrations in the lavages were measured by ELISA, and Nos2 mRNA levels in the peritoneal cells were measured by quantitative (q)RT-PCR. (e) MA or TDM emulsions were intraperitoneally injected into WT mice (n = 4) as described in (d), and peritoneal cells were collected at 48- and 72-h post-injection. Recruitment of neutrophils (CD11b+Ly6G+F4/80−) and monocyte-derived macrophages (CD11b+Ly6G−F4/80low SPMs) was analyzed by flow cytometry. (f, g) WT or Trem2−/− mice were injected intraperitoneally with fMA or control (vehicle) emulsion, peritoneal lavages were collected, and the concentrations of MCP-1 (control, n = 4; fMA, n = 6; at 4 h) and TNF (n = 4; at 72 h) was measured by ELISA (f). Recruitment of peritoneal exudate cells (n = 4; at 72 h) was analyzed as described in (e, g). (h–k) WT mice were injected intraperitoneally with TDM, fMA, or control (vehicle) emulsion, and infiltrated macrophages at days 1, 2, and 3 were analyzed by flow cytometry to measure the expression of the M1 macrophage markers CD38 and iNOS (h). The numbers of total recruited monocyte-derived macrophages (CD11b+Ly6C+F4/80+) (i), the M1 macrophages (CD11b+Ly6C+F4/80+CD38highNOS+) (j), and permissive macrophages (CD11b+Ly6C+F4/80+CD38dullNOS−) (k) at day 3 are shown. Data in (d–k) are presented as the mean ± SEM and are representative of at least three independent experiments. *p < 0.05, **p < 0.01, ***p < 0.001.

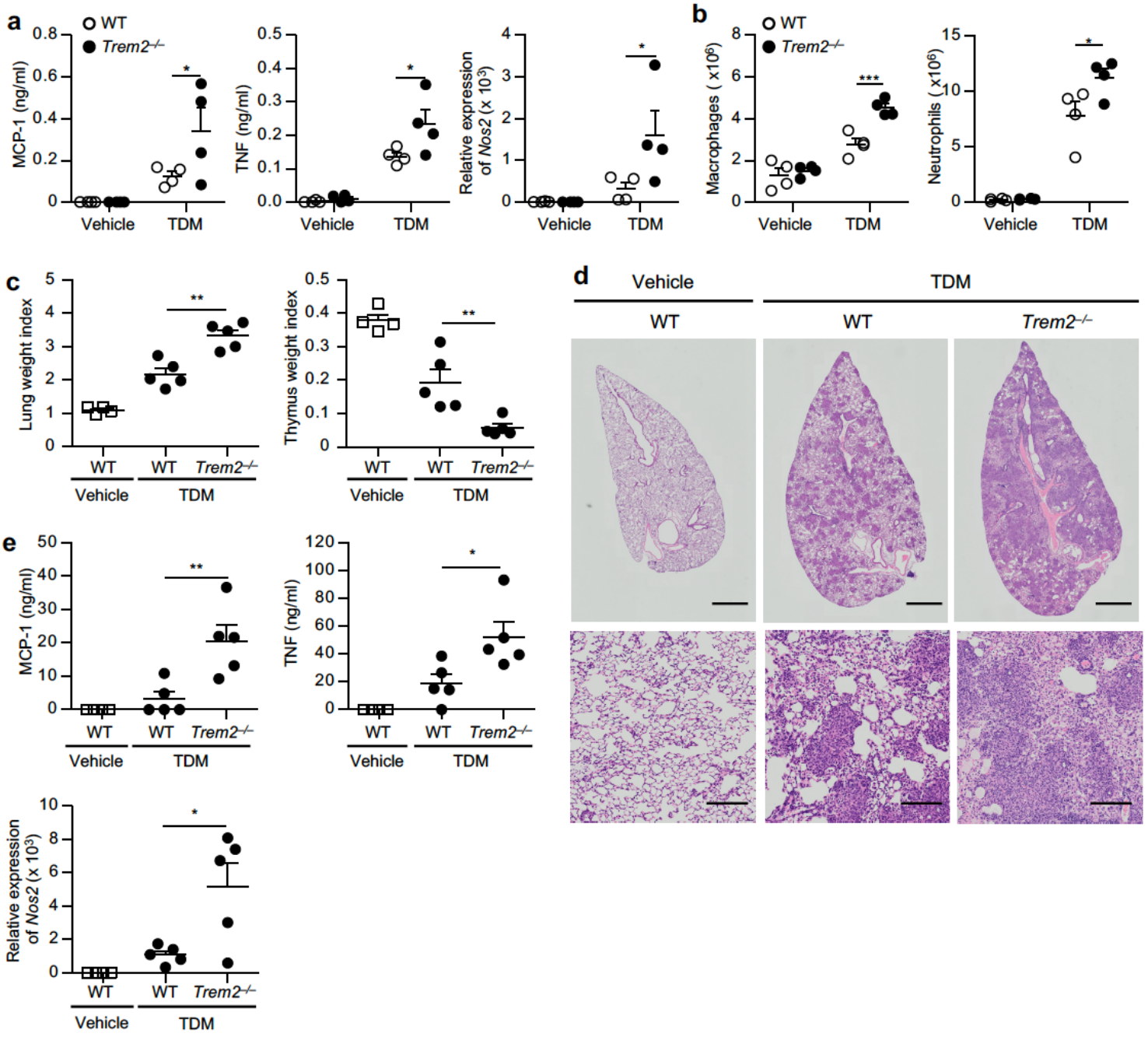

Figure 6

TREM2 deficiency exacerbates Mincle-induced inflammation. (a, b) WT or Trem2−/− mice (n = 4) were intraperitoneally injected with 100 μg TDM or control (vehicle) emulsion. TNF and MCP-1 in the peritoneal lavages were measured by ELISA and Nos2 mRNA levels in the peritoneal cells were measured by qRT-PCR at 24-h post injection (a). The numbers of macrophages and neutrophils in the peritoneal cavities at 72-h post injection were analyzed by flow cytometry (b). (c–e) WT or Trem2−/− mice (n = 5) were intravenously injected with 50 μg TDM or control emulsion, and the lungs and thymuses were collected at day 7 after the injection. LWI and TWI are shown (c). Representative hematoxylin & eosin-stained sections of lung lobes from WT and Trem2−/− mice (scale bars: upper panels, 1 mm; lower panels, 0.1 mm) are

shown (d). Cytokine concentration in lung homogenates was measured by ELISA, and Nos2 mRNA levels in the lungs were measured by qRT-PCR (e). Data in (a–c) and (e) are presented as mean ± SEM and are representative of at least two independent experiments. *p < 0.05, **p < 0.01, ***p < 0.001.

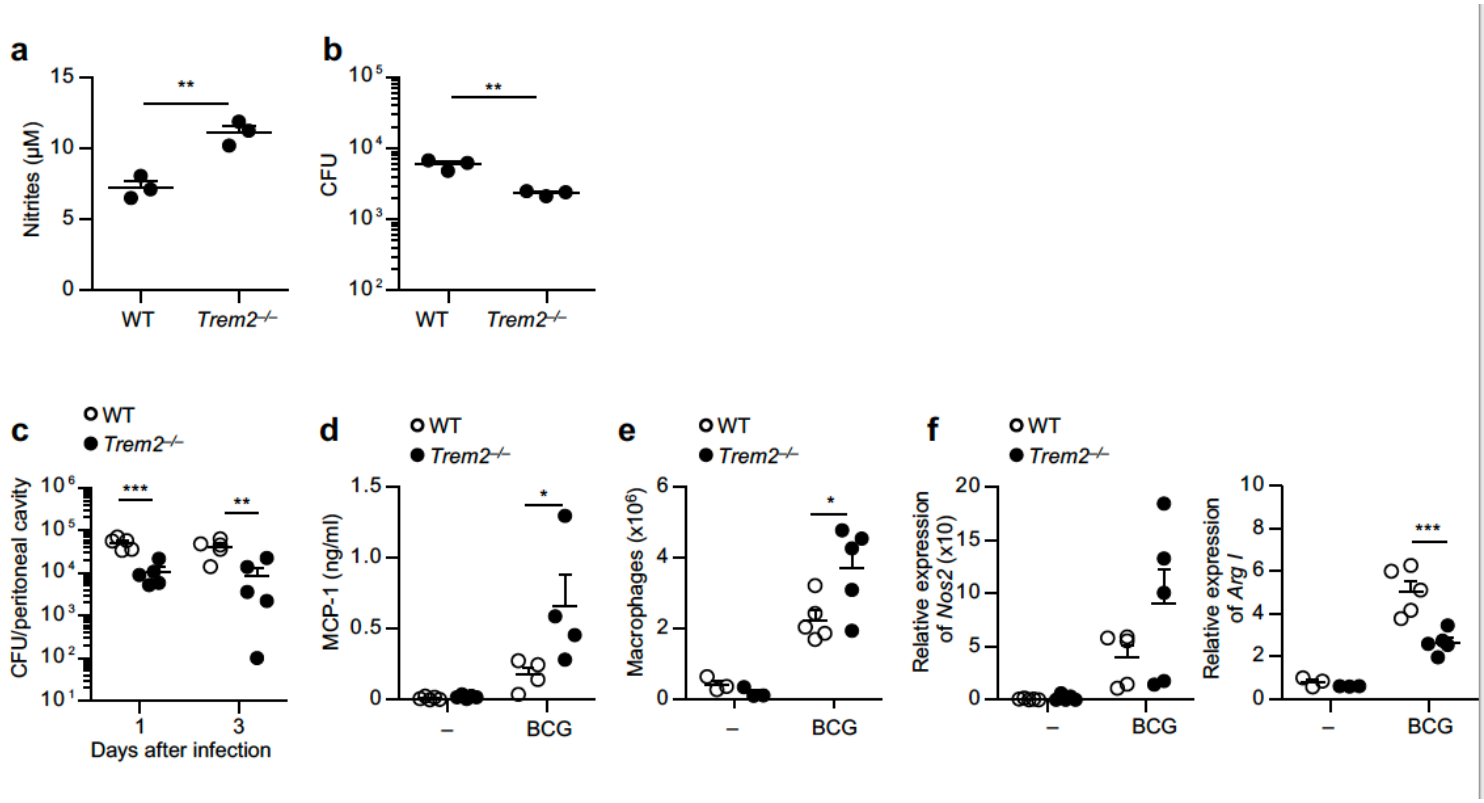

Figure 7

TREM2 deficiency accelerates the clearance of mycobacterial infection. (a, b) WT or Trem2−/− BMDMs were infected in vitro with M. bovis BCG (MOI 10) for 4 h. After washing, the cells were further cultured for 24 h, and nitrite concentration in the culture supernatant was measured by Griess assay (a). The cells were collected, lysed, and CFUs of M. bovis BCG were counted (b). (c–f) WT or Trem2 −/− mice (n = 5) were infected intraperitoneally with 5.0 × 106 CFU of M. bovis BCG. Peritoneal cells were collected at days 1 and 3 after infection and CFUs were determined (c). At 4-h post-infection, peritoneal lavages were collected from uninfected control (−; n = 4) and infected mice (BCG; n = 5) for MCP-1 measurement by ELISA (d).Peritoneal cells (−; n = 3; BCG, n = 5) were collected at day 3 after infection, the numbers of recruited macrophages (CD11b+Ly6C+F4/80+) were determined by flow cytometry (e), and Nos2 mRNA levels were determined by qRT-PCR (f). Data are presented as the mean ± SEM and are representative of two independent experiments. *p < 0.05, **p < 0.01, ***p < 0.001.

Supplementary Files

This is a list of supplementary files associated with this preprint. Click to download.

- Supplementalinfo.pdf